Path-Dependent Constrained Formation for a Quadrotor Team

Zhongjun Hu¹⁰ and Xu Jin¹⁰, Member, IEEE

 $n_{\rho Ji}, n_{h\bar{J}i}, n_{\mu Ji}, \\ \sigma_{mi}, \sigma_{\mu mi},$

 $\sigma_{\rho Ji}, \sigma_{h\bar{J}i}, \sigma_{\mu Ji},$

Abstract—Constrained formation problems, for quadrotors and other systems, have been examined in various works in the past decade. Nevertheless, most works only consider constant or time-varying constraint functions, to be best of our knowledge. In this work, we examine path-dependent constraint requirements during formation tracking operations by a team of quadrotors, where the constraints are functions on path parameters. Universal barrier functions are used to deal with path-dependent constraint requirements, including constraints on distances with desired paths and inter-vehicle distances. Furthermore, unknown quadrotor's mass, inertia, and disturbances are addressed using an adaptive robust formation algorithm. The newly proposed path-dependent constrained formation architecture can ensure formation tracking errors converge exponentially to small neighborhoods near the equilibrium, with all path-dependent constraint requirements met. At the end, a simulation study further illustrates the proposed scheme and demonstrates its

Index Terms—Path-dependent constraints, path-following formation, multi-vehicle system, quadrotors, robust formation tracking.

NOMENCLATURE

d_{ei}	$d_{\mathrm{e}i}$	\triangleq	$ p_i $	$-p_{\mathrm{d}i} ,$	<i>i</i> th	quadrotor	(i	=
	$1, \cdots$,	N) dis	stance to	racki	ng error.		

$$d_{\varepsilon ei}$$
 $d_{\varepsilon ei} \triangleq d_{ei} - 2\varepsilon_{ei}$, ε_{ei} being an arbitrarily small positive constant.

$$d_{ij}$$
 $d_{ij} \triangleq ||p_i - p_j||$, distance between the *i*th and *j*th quadrotors $(i = 1, \dots, N, j \in \mathcal{N}_i)$.

$$d_{eij} = d_{eij} \triangleq d_{ij} - L_{ij}$$
, relative distance tracking error between the *i*th and *j*th quadrotors.

$$E_{dij} = E_{dij} \triangleq \frac{1}{d_{ij}}(p_i - p_j)$$
, unit vector from the jth quadrotor to the ith quadrotor.

$$E_{ei}$$
 $E_{ei} \triangleq \frac{1}{d_{ei}}(p_i - p_{di})$, unit vector from the *i*th quadrotor's desired path to the *i*th quadrotor

$$E_{Lij} \stackrel{\triangle}{=} \frac{1}{L_{ij}} (p_{di} - p_{dj})$$
, unit vector from the *j*th quadrotor's desired path to the *i*th quadrotor's desired path.

$$e_z \qquad e_z \triangleq [0, 0, 1]^{\mathrm{T}}.$$

Received 25 March 2023; revised 26 December 2023 and 2 July 2024; accepted 10 October 2024. This work was supported in part by the National Science Foundation under Grant 2131802 and Grant 2336189. The Associate Editor for this article was T. Q. Dinh. (Corresponding author: Xu Jin.)

The authors are with the Department of Mechanical and Aerospace Engineering, University of Kentucky, Lexington, KY 40506 USA (e-mail: ZhongjunHu@uky.edu; xu.jin@uky.edu).

Digital Object Identifier 10.1109/TITS.2024.3484395

```
Thrust of the ith quadrotor.
                        Gravitational acceleration.
                        Inertia matrix of the ith quadrotor.
K_{ei}, K_{ij}, K_{vi},
                        Positive control gains.
K_{\Theta i}, \nu_{\Theta i}, K_{\omega i},
                        A positive design constant.
                        L_{ij} \triangleq ||p_{di} - p_{dj}||, desired relative dis-
                        tance between the ith and jth quadrotors.
                        Mass of the ith quadrotor.
                        Neighbor set of the ith quadrotor (|\mathcal{N}_i| =
\mathcal{N}_i
N
                        Number of quadrotors (N \ge 3).
                        Adaptive control parameters.
n_{mi}, n_{\mu mi},
```

$p_{\mathrm{d}i}$, $p_{\mathrm{d}j}$	$p_{di}(s_i), p_{dj}(s_j) : \mathbb{R} \to \mathbb{R}^3$, desired
	paths of the i th and j th quadrotors,
	respectively.
p_i, p_i	$p_i \triangleq [x_i, y_i, z_i]^T, p_i \triangleq [x_i, y_i, z_i]^T,$

r to r j	Fi City Sty Cia y F J Cia y S J y Ca y						
	positions of the i th and j th quadrotors.						
s_i	Path parameter for the <i>i</i> th quadrotor.						
$v_{\mathrm{d}i}$	$v_{\mathrm{d}i}(s_i)$: $\mathbb{R} \rightarrow \mathbb{R}$, a desired speed						
	assignment for the <i>i</i> th quadrotor.						
v_i, v_j	Velocities of the <i>i</i> th and <i>j</i> th quadrotors.						

$$\alpha_{pi}, \alpha_{\Theta i}$$
 Stabilizing functions for position and attitude of the *i*th quadrotor.

 γ_{1i}, γ_{2i} Disturbances for the *i*th quadrotor.

$$\eta_{ei}, \eta_{ij}$$
Transformed errors defined in (14).

 $\Theta_i \triangleq [\phi_i, \ \theta_i, \ \psi_i]^T$, attitude of the *i*th quadrotor in the inertial reference frame.

 $\Theta_{di} \triangleq [\phi_{di}, \ \theta_{di}, \ \psi_{di}]^T$, desired attitude

$$\Theta_{di} \stackrel{\triangle}{=} [\phi_{di}, \theta_{di}, \psi_{di}]^{T},$$
 desired attitude of the *i*th quadrotor in the inertial reference frame.

$$au_i$$
 Torques of the *i*th quadrotor.

$$\Omega_{\text{H}i}$$
 $\Omega_{\text{H}i}(s_i): \mathbb{R} \to \mathbb{R}^+$, path-dependent constraint function for d_{ei} .

$$\Omega_{d\mathrm{H}i} \triangleq \Omega_{\mathrm{H}i} - 2\varepsilon_{\mathrm{e}i}, \ \varepsilon_{\mathrm{e}i}$$
 being an arbitrarily small positive constant.

$$\Omega_{\mathrm{H}ij}, \Omega_{\mathrm{L}ij}$$
 $\Omega_{\mathrm{H}ij}(s_i, s_j), \ \Omega_{\mathrm{L}ij}(s_i, s_j) : \mathbb{R} \times \mathbb{R} \to \mathbb{R}^+,$ path-dependent constraint functions for $d_{\mathrm{e}ij}$.

 ω_i Angular velocity of the *i*th quadrotor with respect to the body-fixed frame.

I. Introduction

PORMATION control of unmanned aerial vehicles (UAVs), especially quadrotors, has many practical applications in surveillance [1], [2], search and rescue [3], contour mapping [4], [5], source locating [6], object lifting and transporting [7], [8], [9], [10], [11], just to name a few.

During UAV formations, various motion constraints need to be guaranteed to ensure safety and performance of the system. Common approaches in handling this UAV constrained formation problem include artificial potential fields (APFs) [12], [13], [14], [15], [16], [17], control barrier functions (CBFs) [18], [19], [20], [21], [22], barrier functions/barrier Lyapunov functions (BLFs) [23], [24], [25], [26], [27], [28], and model predictive control (MPC) methods [29], [30], [31], [32], [33]. However, only constant or time-varying constraint functions are discussed in the aforementioned works. In practice, there are often situations in which the constraints are geometric or spatial in nature. For example, for a team of small UAVs to pass through a narrow window, the formation needs to be more compact at the window compared with other locations. In this example, the corresponding constraint requirements on inter-UAV distances are spatial related (where the narrow window is located), regardless of time (when the team is pass through the narrow window). Defining such constraint requirements as functions of time will put unnecessary temporal restrictions on the system dynamics. Therefore, existing constrained formation control algorithms in the literature are not suitable for such path-dependent constrained formation requirements.

Very recently, we have proposed a path-dependent constrained control algorithm for an autonomous vehicle on a 2-D plane [34], where path-dependent constrained requirements can be satisfied during operation. However, [34] focuses on the operation of a single vehicle on a 2-D plane, hence not suitable for multiple UAVs formation in a 3-D space.

In this paper, for the first time in the formation control literature, we investigate path-dependent constraints for UAV formation operations. This is in contrast to most existing works in the literature that can only handle constant or at best time-varying constraint requirements, which can be conservative in constraint formulation and cannot respond well to the operation environment. First, for the performance constraints, the distance between each quadrotor and its desired path should not be too large. Second, for the safety constraints, we need to guarantee that the relative distance between any two quadrotors cannot be either too small or too large. The main technical difficulty is the fact that the constraint requirements are not directly depending on the time variable. The design is further complicated by system unknown parameters and disturbances. To address these difficulties, a path parameter timing law is designed and integrated into the constrained formation control law, which updates path parameters based on system states. This timing law serves as a bridge between the temporal vehicle dynamics and the geometric/spatial constraint requirements. We adopt universal barrier functions to address path-dependent constraints in this paper. The newly proposed path-dependent constrained formation architecture can ensure formation tracking errors converge exponentially

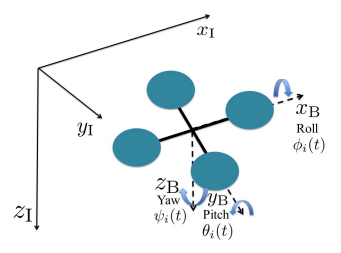


Fig. 1. Illustration of the inertial {I} and body-fixed {B} frames.

to arbitrarily small neighborhoods near the equilibrium, with all path-dependent constraint requirements met.

We will use the following standard notations in this paper. First, \mathbb{R} is real number set, \mathbb{R}^+ is positive real number set, and I_m denotes the $m \times m$ identity matrix. Moreover, $(\cdot)^T$ is the transpose of (\cdot) , $|\cdot|$ represents the absolute value for scalars, and $||\cdot||$ represents the Euclidean norm for vectors and induced norm for matrices. Furthermore, we use $c\theta$ to denote $\cos\theta$, $s\theta$ to denote $\sin\theta$, and $t\theta$ to denote $\tan\theta$. We also write (\cdot) as the first order time derivative of (\cdot) , if (\cdot) is differentiable. Besides, for any two vectors $v_1, v_2 \in \mathbb{R}^3$, the cross-product operator $\mathbb{S}(\cdot)$ gives $\mathbb{S}(v_1)v_2 = v_1 \times v_2$. It is also true that $\mathbb{S}(v_1)v_2 = -\mathbb{S}(v_2)v_1$ and $v_1^T\mathbb{S}(v_2)v_1 = 0$. Finally, $SO(3) = \{X \in \mathbb{R}^{3 \times 3}: X^TX = I_3\}$ is a set of orthogonal matrices in $\mathbb{R}^{3 \times 3}$, and $S^2 = \{x \in \mathbb{R}^3: ||x|| = 1\}$ is a set of unit vectors in \mathbb{R}^3 .

II. PROBLEM FORMULATION

A. Basic Graph Theory and Notations

A weighted undirected graph is represented by $\mathcal{G} = (\mathcal{V}, \mathcal{E})$, where $\mathcal{V} = \{1, \cdots, N\}$ is a nonempty set of nodes/agents, and $\mathcal{E} \subset \mathcal{V} \times \mathcal{V}$ is the set of edges/arcs. $(j,i) \in \mathcal{E}$ implies that agent i can receive information from its neighboring agent j, and vice versa. In this case, agent j is called a neighbor of agent i. Furthermore, \mathcal{N}_i denotes the set of neighbors of agent i and $|\mathcal{N}_i|$ represents the number of neighbors. In this work, we consider the scenario where $|\mathcal{N}_i| = 2$. The topology of a weighted graph \mathcal{G} is often represented by the adjacency matrix $\mathcal{A} = [a_{ij}] \in \mathbb{R}^{N \times N}$, where $a_{ij} = 1$ if $(j,i) \in \mathcal{E}$; otherwise $a_{ij} = 0$. It is assumed that $a_{ii} = 0$, and the topology is fixed, i.e., \mathcal{A} is time invariant. Define $\bar{a}_i = \sum_{j=1}^N a_{ij}$ as the weighted in-degree of node i and $\bar{\mathcal{A}} = \operatorname{diag}(\bar{a}_1, \cdots, \bar{a}_N) \in \mathbb{R}^{N \times N}$ as the in-degree matrix. The graph Laplacian matrix is $\mathcal{L} = \bar{\mathcal{A}} - \mathcal{A} \in \mathbb{R}^{N \times N}$.

B. System Dynamics

Consider a group of N quadrotors $(N \ge 3)$, where, for the ith quadrotor $(i = 1, \dots, N)$ shown in Figure 1, the position and attitude in the inertial reference frame are represented as $p_i(t) \triangleq [x_i(t), y_i(t), z_i(t)]^T \in \mathbb{R}^3$ and $\Theta_i(t) \triangleq [\phi_i(t), \theta_i(t), \psi_i(t)]^T \in \mathbb{R}^3$, respectively. The translational velocity with respect to the inertial reference frame is represented as $v_i(t) \in \mathbb{R}^3$. Moreover, define a body-fixed frame with the origin being at the center of mass for each quadrotor, and the angular velocity with respect to this body-fixed frame is denoted by $\omega_i(t) \triangleq [\omega_{xi}(t), \omega_{yi}(t), \omega_{zi}(t)]^T \in \mathbb{R}^3$. The

kinematics for the ith quadrotor are expressed as

$$\dot{p}_i(t) = v_i(t),\tag{1}$$

$$\dot{\Theta}_i(t) = T(\Theta_i(t))\omega_i(t), \tag{2}$$

where $p_i(0) = p_{i0} \in \mathbb{R}^3$ and $\Theta_i(0) = \Theta_{i0} \in \mathbb{R}^3$, with p_{i0} and Θ_{i0} being initial conditions. Besides, $T(\Theta_i(t))$ is a transformation matrix [35] that relates the angular velocity in the body-fixed frame to the rate of change of Euler angles in the inertial frame, and is given by

$$T(\Theta_i) = \begin{bmatrix} 1 & s\phi_i t\theta_i & c\phi_i t\theta_i \\ 0 & c\phi_i & -s\phi_i \\ 0 & s\phi_i/c\theta_i & c\phi_i/c\theta_i \end{bmatrix},$$
(3)

where we have $||T(\Theta_i(t))|| \leq T_{\max}$, with $T_{\max} > 0$ being a known constant, when $-\frac{\pi}{2} < \phi_i(t) < \frac{\pi}{2}$ and $-\frac{\pi}{2} < \theta_i(t) < \frac{\pi}{2}$. The ith quadrotor $(i = 1, \cdots, N)$ system dynamics are

The *i*th quadrotor $(i = 1, \dots, N)$ system dynamics are represented by

$$m_i \dot{v}_i(t) = m_i g e_z - F_i R(\Theta_i(t)) e_z + \gamma_{1i}(t), \tag{4}$$

$$J_i \dot{\omega}_i(t) = \mathbb{S}(J_i \omega_i(t)) \omega_i(t) + \tau_i(t) + \gamma_{2i}(t), \tag{5}$$

where $v_i(0) = v_{i0} \in \mathbb{R}^3$ and $\omega_i(0) = \omega_{i0} \in \mathbb{R}^3$. $m_i \in \mathbb{R}$, $m_i > 0$ is the mass of the *i*th quadrotor $(i = 1, \dots, N)$, and $J_i \in \mathbb{R}^{3 \times 3}$ is a symmetric positive definite matrix representing the inertia of the *i*th quadrotor. $F_i(t) \in \mathbb{R}$ and $\tau_i(t) \in \mathbb{R}^3$ represent the thrust and torques of the *i*th quadrotor, respectively. $\gamma_{1i}(t) \in \mathbb{R}^3$ and $\gamma_{2i}(t) \in \mathbb{R}^3$ denote the external disturbances. Furthermore, $g \in \mathbb{R}$ is the gravitational acceleration and $e_z = [0, 0, 1]^T \in S^2$ is a unit vector. $R(\Theta_i(t)) \in SO(3)$ is a rotation matrix [35], which translates the translational velocity vector in the body-fixed frame into the rate of change of the position vector in the inertial frame

 $R(\Theta_i)$

$$= \begin{bmatrix} c\theta_i c\psi_i & as\phi_i s\theta_i c\psi_i - c\phi_i s\psi_i & c\phi_i s\theta_i c\psi_i + s\phi_i s\psi_i \\ c\theta_i s\psi_i & s\phi_i s\theta_i s\psi_i + c\phi_i c\psi_i & c\phi_i s\theta_i s\psi_i - s\phi_i c\psi_i \\ -s\theta_i & s\phi_i c\theta_i & c\phi_i c\theta_i \end{bmatrix}$$
(6)

C. Performance and Safety Constraints

The coordinate of the desired path for the *i*th quadrotor $(i = 1, \dots, N)$ $p_{di}(s_i) : \mathbb{R} \to \mathbb{R}^3$ is denoted by $p_{di}(s_i) \triangleq [x_{di}(s_i), y_{di}(s_i), z_{di}(s_i)]^T \in \mathbb{R}^3$, where $s_i \in \mathbb{R}$ is a path parameter of the *i*th quadrotor, and $p_{di}(s_i)$ is chosen to be at least three-times continuously differentiable with bounded derivatives. Note that $p_{di}(s_i)$ is any *arbitrary* point on the desired path, not necessarily the vehicle's closest/projection point on the desired path.

The distance tracking error $d_{ei}(t, s_i)$ for the *i*th quadrotor is defined as

$$d_{\mathrm{e}i}(t,s_i) \triangleq ||p_i(t) - p_{\mathrm{d}i}(s_i)||. \tag{7}$$

Furthermore, the desired relative distance between the *i*th and *j*th $(i = 1, \dots, N, j \in \mathcal{N}_i)$ quadrotors is defined as

$$L_{ij}(s_i, s_j) \triangleq \left| \left| p_{di}(s_i) - p_{dj}(s_j) \right| \right|, \tag{8}$$

and the actual relative distance is given by

$$d_{ij}(t) \triangleq \left| \left| p_i(t) - p_j(t) \right| \right|. \tag{9}$$

During the formation tracking task, there are *performance* and *safety* constraint requirements that need to be satisfied. First, for $i=1,\cdots,N$, let $\Omega_{\mathrm{H}i}(s_i):\mathbb{R}\to\mathbb{R}^+$ be uniformly bounded and at least three-times continuously differentiable with bounded derivatives, and $d_{\mathrm{e}i}(0,s_i(0))<\Omega_{\mathrm{H}i}(s_i(0))$. The distance tracking error for the ith quadrotor $d_{\mathrm{e}i}(t,s_i)$ ($i=1,\cdots,N$) has to satisfy the following *performance constraint*

$$d_{ei}(t, s_i) < \Omega_{Hi}(s_i). \tag{10}$$

From (7), $d_{ei}(t, s_i) \ge 0$ at all time. However, in order to avoid singularity in the controller later in the analysis, it is needed for $d_{ei}(t, s_i)$ to be bounded away from the origin. Thus, the constraint requirement (10) is modified as

$$0 < \varepsilon_{ei} < d_{ei}(t, s_i) < \Omega_{Hi}(s_i), \tag{11}$$

where ε_{ei} is any arbitrarily small positive constant. Note that (11) is equivalent to

$$-\varepsilon_{ei} < d_{\varepsilon ei}(t, s_i) < \Omega_{dHi}(s_i), \tag{12}$$

where $d_{\varepsilon ei}(t, s_i) \triangleq d_{ei}(t, s_i) - 2\varepsilon_{ei}$ and $\Omega_{dHi}(s_i) \triangleq \Omega_{Hi}(s_i) - 2\varepsilon_{ei}$.

Remark 1: An example for $\Omega_{Hi}(s_i)$ can be

$$\Omega_{\text{H}i}(s_i) = d_{\text{e}i}(0, s_i(0))e^{-\alpha_{\text{H}i}(s_i - s_i(0))^2} + \Omega_{\text{H}i\infty},$$

where $\alpha_{\mathrm{H}i} > 0$ is a selected constant to determine the convergent speed of this constraint function, and $\Omega_{\mathrm{H}i\infty} > 2\varepsilon_{\mathrm{e}i}$. Such a selection of $\Omega_{\mathrm{H}i}(s_i)$ tolerates a relatively larger initial distance tracking error, but puts a tighter requirement on the distance tracking error as the operation continues.

Remark 2: In the analysis to be presented later, we will show that the distance tracking error $d_{ei}(t, s_i)$ will converge to a small neighbourhood of $2\varepsilon_{ei}$, which is a shifted equilibrium point bounded away from zero. This equilibrium shift method to avoid singularity in the control design is common in the literature [36], [37], [38]. More discussion on how the modified constraint requirement (12) can help avoid singularity in the control design can be seen in the later Remark 10.

Second, define the relative distance tracking error between the ith and jth quadrotors ($i=1,\cdots,N,$ $j\in\mathcal{N}_i$) as $d_{eij}(t,s_i,s_j)\triangleq d_{ij}(t)-L_{ij}(s_i,s_j)$. Let $\Omega_{\mathrm{H}ij}(s_i,s_j),\ \Omega_{\mathrm{L}ij}(s_i,s_j):\mathbb{R}\times\mathbb{R}\to\mathbb{R}^+$ be uniformly bounded and at least three-times continuously differentiable with bounded partial derivatives, and $-\Omega_{\mathrm{L}ij}(s_i(0),s_j(0))< d_{\mathrm{e}ij}(0,s_i(0),s_j(0))< d_{\mathrm{H}ij}(s_i(0),s_j(0))$. The safety constraint is

$$-\Omega_{Lij}(s_i, s_j) < d_{eij}(t, s_i, s_j) < \Omega_{Hij}(s_i, s_j),$$
 (13)

which requires that the inter-quadrotor distance cannot be either too large or too small. For instance, when quadrotors need to exchange information for coordination, the distances between them should be within the effective communication range. Besides, too small inter-quadrotor distance may lead to collisions between quadrotors.

Remark 3: An example for $\Omega_{\text{H}ij}(s_i, s_j)$ and $\Omega_{\text{L}ij}(s_i, s_j)$ can be

$$\begin{split} \Omega_{\mathrm{H}ij}(s_i,s_j) &= |d_{\mathrm{e}ij}(0,s_i(0),s_j(0))| \left[\delta_{ij} \mathrm{e}^{-\alpha_{\mathrm{H}ij}(s_i - s_i(0))^2} \right. \\ &+ (1 - \delta_{ij}) \mathrm{e}^{-\alpha_{\mathrm{H}ij}(s_j - s_j(0))^2} \right] + \Omega_{\mathrm{H}ij\infty}, \\ \Omega_{\mathrm{L}ij}(s_i,s_j) &= |d_{\mathrm{e}ij}(0,s_i(0),s_j(0))| \left[\delta_{ij} \mathrm{e}^{-\alpha_{\mathrm{L}ij}(s_i - s_i(0))^2} \right. \\ &+ (1 - \delta_{ij}) \mathrm{e}^{-\alpha_{\mathrm{L}ij}(s_j - s_j(0))^2} \right] + \Omega_{\mathrm{L}ij\infty}, \end{split}$$

where $\alpha_{\text{H}ij} > 0$ and $\alpha_{\text{L}ij} > 0$ are selected to determine convergent speeds of safety constraint functions. Moreover, $\Omega_{\text{H}ij\infty}$, $\Omega_{\text{L}ij\infty} > 0$, and $0 < \delta_{ij} < 1$. In this example, $\Omega_{\text{H}ij}(s_i, s_j)$ and $\Omega_{\text{L}ij}(s_i, s_j)$ tolerate a relatively larger initial distance tracking error, but put a tighter requirement on the relative distance tracking error as the operation continues.

D. Control Objective

The **control objective** for the path-following formation tracking problem is to design a control framework such that:

- 1) The distance tracking error $d_{ei}(t, s_i)$ for the *i*th quadrotor $(i = 1, \dots, N)$ can converge into an arbitrarily small neighborhood of the equilibrium;
- 2) The relative distance tracking error $d_{eij}(t, s_i, s_j)$ between the *i*th and *j*th $(i = 1, \dots, N, j \in \mathcal{N}_i)$ quadrotors can converge into an arbitrarily small neighborhood of zero;
- 3) For the *i*th quadrotor $(i = 1, \dots, N)$, the attitude tracking error $e_{\Theta i} \triangleq [e_{\phi i}, e_{\theta i}, e_{\psi i}]^{T} = \Theta_{i} \Theta_{di}$ can converge into an arbitrarily small neighborhood of zero, where $\Theta_{di} \triangleq [\phi_{di}, \theta_{di}, \psi_{di}]^{T}$ is the desired attitude to be specified later;
- 4) The path speed error $z_{si} \triangleq \dot{s}_i v_{di}(s_i)$, can converge into an arbitrarily small neighborhood of zero, where $v_{di}(s_i) : \mathbb{R} \rightarrow \mathbb{R}$ is at least twice continuously differentiable with bounded derivatives;
- 5) The path-dependent performance and safety constraint requirements (12) and (13) will not be violated during formation

Remark 4: Note that the constraint requirements (12) and (13) depend on the path parameters s_i ($i = 1, \dots, N$) instead of the time variable t directly. The physical meaning behind this new constraint formulation is that the constraint requirements are geometrically/spatially related, not temporally defined. Similar to the control structures in [39] and [40], timing laws will be introduced to connect these path-dependent constraint requirements and temporal vehicle dynamics.

Define the unit vector between the ith quadrotor and its desired path as E_{ei} ($i=1,\cdots,N$) and unit vectors between the ith quadrotor and its neighboring agents E_{dij} ($j\in\mathcal{N}_i$) as $E_{ei}\triangleq\frac{1}{d_{ei}}(p_i-p_{di})\in S^2$ and $E_{dij}\triangleq\frac{1}{d_{ij}}(p_i-p_j)\in S^2$. We will need the following assumptions for the analysis and discussion of our main theoretical results.

Assumption 1: In this work, the system states including position, velocity, attitude, and angular velocity can be accurately measured for the controller design.

Remark 5: Addressing safety and performance constraints with measurement uncertainties is in general a difficult task. For example, if the system is subject to stochastic noise, the constraint requirements can only be defined in terms of probability, as in our prior work [41]. For the benefit of discussion and to focus our main contributions on path-dependent

constrained formation, sensor uncertainties are beyond the scope of this work.

Assumption 2: For the *i*th quadrotor $(i = 1, \dots, N)$, the unit vectors E_{ei} and E_{dij} $(j \in \mathcal{N}_i)$ are not coplanar.

Remark 6: Geometrically, Assumption 2 requires that the 3D UAV formation problem should not be reduced onto a 2D plane for any agent at all time. More discussion can be seen in Remark 11.

Assumption 3: For the reference attitude of the *i*th quadrotor, we require that $\phi_{di} \in (-\frac{\pi}{2}, \frac{\pi}{2})$, $\theta_{di} \in (-\frac{\pi}{2}, \frac{\pi}{2})$, and $\psi_{di} \in [-\pi, \pi]$, where ψ_{di} is at least once continuously differentiable with bounded $\dot{\psi}_{di}$.

Assumption 4 ([25], [42], [43]): The thrust F_i and external disturbances γ_{1i} and γ_{2i} for the *i*th quadrotor are uniformly bounded with *unknown* bounds.

Assumption 5 ([42]): The mass m_i and inertia J_i for the ith quadrotor are $\underline{unknown}$, and the inverse of J_i is assumed to be bounded, such that for any $z \in \mathbb{R}^3$, $\underline{b}_{Ji}z^Tz \leq z^TJ_i^{-1}z \leq \overline{b}_{Ji}z^Tz$, where \overline{b}_{Ji} and \underline{b}_{Ji} are $\underline{unknown}$ positive constants.

Assumption 6 ([25]): The attitude of the *i*th quadrotor is confined such that $\phi_i \in (-\frac{\pi}{2}, \frac{\pi}{2}), \theta_i \in (-\frac{\pi}{2}, \frac{\pi}{2}), \text{ and } \psi_i \in [-\pi, \pi].$

Remark 7: The boundedness of ϕ_i and θ_i guarantees that $T(\Theta_i)$ given in (3) is invertible during the operation.

III. UNIVERSAL BARRIER FUNCTION

Here we introduce the structure of universal barrier function (UBF) [44] to address the issue of path-dependent constraint requirements. Specifically, the following transformed error variables are introduced

$$\eta_{ei} = \frac{\Omega_{dHi} d_{\epsilon ei}}{(\Omega_{dHi} - d_{\epsilon ei})(\varepsilon_{ei} + d_{\epsilon ei})},$$

$$\eta_{ij} = \frac{\Omega_{Hij} \Omega_{Lij} d_{eij}}{(\Omega_{Hij} - d_{eij})(\Omega_{Lij} + d_{eij})}.$$
(14)

The universal barrier functions used to deal with the constraint requirements (12) and (13) for the ith agent are then designed as

$$V_{ei} = \frac{1}{2}\eta_{ei}^2, \quad V_{ij} = \frac{1}{2}\eta_{ij}^2.$$
 (15)

Remark 8: Compared with widely used BLFs, such as logtype BLF [45] and tan-type BLF [46], the UBF first transforms the original state with the constraint requirement into an unconstrained one. Next, by keeping the UBF uniformly bounded through closed-loop analysis, the transformed error variable will also become bounded, therefore, the constraint requirement can be guaranteed. UBFs can also deal with symmetric and asymmetric constraints in a unified framework. Due to the page limit, more details can refer to our earlier work [44].

Remark 9: The UBF approach employed in this work differs fundamentally from CBF-based approaches in the following three aspects: 1) Computational demands: CBF approaches are optimization-based algorithms that demand significant computational power, which is often unrealistic for small UAV platforms; 2) Analytic solutions: Unlike CBF frameworks, which do not offer analytical solutions, our algorithm provides explicit analytical controllers; 3) Feasibility

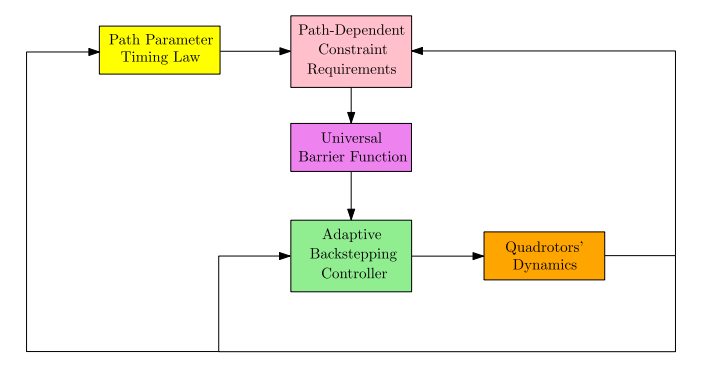


Fig. 2. High-level block diagram of the overall control framework.

concerns: Unlike UBF approaches, optimization-based algorithms face feasibility problems, as feasible solutions may or may not exist.

IV. CONTROL DESIGN AND MAIN RESULTS

First, to provide a brief overview of the proposed control framework, we present a high-level block diagram as Figure 2.

The following lemma is needed for the controller design and theoretical analysis to be presented.

Lemma 1 ([47]): For any constant $\varepsilon > 0$ and any variable $z \in \mathbb{R}$, we have $0 \le |z| - \frac{z^2}{\sqrt{z^2 + \varepsilon^2}} < \varepsilon$.

Detailed analysis is as follows.

A. Distance Control Design and Results

Step 1

At this step, we consider the position kinematics of the quadrotors. Let $V_1 = \sum_{i=1}^{N} \left(V_{ei} + \sum_{j \in \mathcal{N}_i} V_{ij}\right)$, its derivative with respect to time leads to

$$\dot{V}_1 = \sum_{i=1}^{N} \left(\eta_{ei} \dot{\eta}_{ei} + \sum_{i \in \mathcal{N}_i} \eta_{ij} \dot{\eta}_{ij} \right). \tag{16}$$

First we examine the dynamics for η_{ei} $(i = 1, \dots, N)$. From (14), we have

$$\dot{\eta}_{ei} = \frac{\partial \eta_{ei}}{\partial s_i} \dot{s}_i + \frac{\partial \eta_{ei}}{\partial d_{eei}} E_{ei}^{\mathrm{T}} \dot{p}_i, \tag{17}$$

where

$$\begin{split} \frac{\partial \eta_{ei}}{\partial s_{i}} &= \frac{\partial \eta_{ei}}{\partial \Omega_{dHi}} \frac{d\Omega_{dHi}}{ds_{i}} - \frac{\partial \eta_{ei}}{\partial d_{\epsilon ei}} E_{ei}^{T} \frac{dp_{di}}{ds_{i}} \in \mathbb{R}, \\ \frac{\partial \eta_{ei}}{\partial d_{\epsilon ei}} &= \frac{\Omega_{dHi} (\Omega_{dHi} \varepsilon_{ei} + d_{\epsilon ei}^{2})}{(\Omega_{dHi} - d_{\epsilon ei})^{2} (\varepsilon_{ei} + d_{\epsilon ei})^{2}} > 0. \end{split}$$

Hence for \dot{V}_{ei} $(i = 1, \dots, N)$ we get

$$\dot{V}_{ei} = \eta_{ei} \frac{\partial \eta_{ei}}{\partial s_i} \dot{s}_i + \eta_{ei} \frac{\partial \eta_{ei}}{\partial d_{sei}} E_{ei}^{\mathrm{T}} \dot{p}_i. \tag{18}$$

Similarly, for \dot{V}_{ij} $(i = 1, \dots, N, j \in \mathcal{N}_i)$ we obtain

$$\dot{V}_{ij} = \eta_{ij} \frac{\partial \eta_{ij}}{\partial s_i} \dot{s}_i + \eta_{ij} \frac{\partial \eta_{ij}}{\partial s_j} \dot{s}_j
+ \eta_{ij} \frac{\partial \eta_{eij}}{\partial d_{eij}} E_{dij}^{\mathrm{T}} (\dot{p}_i - \dot{p}_j),$$
(19)

where

$$\begin{split} \frac{\partial \eta_{ij}}{\partial s_{i}} &= \frac{\partial \eta_{ij}}{\partial \Omega_{\mathrm{H}ij}} \frac{\partial \Omega_{\mathrm{H}ij}}{\partial s_{i}} + \frac{\partial \eta_{ij}}{\partial \Omega_{\mathrm{L}ij}} \frac{\partial \Omega_{\mathrm{L}ij}}{\partial s_{i}} \\ &- \frac{\partial \eta_{ij}}{\partial d_{\mathrm{e}ij}} E_{\mathrm{L}ij}^{\mathrm{T}} \frac{\mathrm{d}p_{\mathrm{d}i}}{\mathrm{d}s_{i}} \in \mathbb{R}, \\ \frac{\partial \eta_{ij}}{\partial s_{j}} &= \frac{\partial \eta_{ij}}{\partial \Omega_{\mathrm{H}ij}} \frac{\partial \Omega_{\mathrm{H}ij}}{\partial s_{j}} + \frac{\partial \eta_{ij}}{\partial \Omega_{\mathrm{L}ij}} \frac{\partial \Omega_{\mathrm{L}ij}}{\partial s_{j}} \\ &+ \frac{\partial \eta_{ij}}{\partial d_{\mathrm{e}ij}} E_{\mathrm{L}ij}^{\mathrm{T}} \frac{\mathrm{d}p_{\mathrm{d}j}}{\mathrm{d}s_{j}} \in \mathbb{R}, \\ E_{\mathrm{L}ij} &\triangleq \frac{1}{L_{ij}} (p_{\mathrm{d}i} - p_{\mathrm{d}j}) \in S^{2}, \\ \frac{\partial \eta_{ij}}{\partial d_{\mathrm{e}ij}} &= \frac{\Omega_{\mathrm{H}ij} \Omega_{\mathrm{L}ij} (\Omega_{\mathrm{H}ij} \Omega_{\mathrm{L}ij} + d_{\mathrm{e}ij}^{2})}{(\Omega_{\mathrm{H}ij} - d_{\mathrm{e}ij})^{2} (\Omega_{\mathrm{L}ij} + d_{\mathrm{e}ij})^{2}} > 0. \end{split}$$

Hence, from (16), \dot{V}_1 yields to

$$\dot{V}_{1} = \sum_{i=1}^{N} \left(\Pi_{pi}^{T} \Lambda_{pi} E_{pi}^{T} v_{i} + \Pi_{pi}^{T} g_{si} \dot{s}_{i} \right), \tag{20}$$

where

$$\Pi_{pi} \triangleq \begin{bmatrix} \eta_{ei}, & \underline{\eta_{ij}} \\ j \in \mathcal{N}_i \end{bmatrix}^{\mathrm{T}} \in \mathbb{R}^3,
\Lambda_{pi} \triangleq \operatorname{diag} \left(\frac{\partial \eta_{ei}}{\partial d_{\varepsilon ei}}, & 2 \frac{\partial \eta_{ij}}{\partial d_{eij}} \right) \in \mathbb{R}^{3 \times 3},
E_{pi} \triangleq \begin{bmatrix} E_{ei}, & \underline{E_{dij}} \\ j \in \mathcal{N}_i \end{bmatrix} \in \mathbb{R}^{3 \times 3}, \quad g_{si} \triangleq \begin{bmatrix} \frac{\partial \eta_{ei}}{\partial s_i}, & 2 \frac{\partial \eta_{ij}}{\partial s_i} \end{bmatrix}^{\mathrm{T}} \in \mathbb{R}^3.$$

Next, define the fictitious velocity tracking error as $e_{vi} = E_{pi}^{T} v_i - \alpha_{pi}$, with the stabilizing function $\alpha_{pi} \in \mathbb{R}^3$ $(i = 1, \dots, N)$ designed as

$$\alpha_{pi} = -\Lambda_{pi}^{-1}(g_{si}v_{di} + K_i\Pi_{pi}),$$
 (21)

where $K_i \triangleq \operatorname{diag}(K_{ei}, \underbrace{K_{ij}}_{j \in \mathcal{N}_i})$ in which $K_{ei} > 0$ and $K_{ij} > 0$

are the control gains. Besides, since Λ_{pi} is a diagonal matrix with positive diagonal entries, Λ_{pi} is invertible and $\Lambda_{pi}^{-1} = \operatorname{diag}\left(\frac{1}{\frac{\partial \eta_{ei}}{\partial d_{eei}}}, \frac{1}{2\frac{\partial \eta_{ij}}{\partial d_{eij}}}\right)$. Thus, the proposed stabilizing function

 α_{pi} in (21) is non-singular. Hence, (20) yields

$$\dot{V}_{1} = \sum_{i=1}^{N} \left(\Pi_{pi}^{T} \Lambda_{pi} e_{vi} - K_{ei} \eta_{ei}^{2} - \sum_{j \in \mathcal{N}_{i}} K_{ij} \eta_{ij}^{2} + \Pi_{pi}^{T} g_{si} z_{si} \right).$$
(22)

Step 2

At this step, we consider the translational dynamics of the quadrotors. Let $V_2 = \sum_{i=1}^{N} \frac{1}{2} e_{vi}^{T} e_{vi}$, and its time derivative

gives

$$\dot{V}_{2} = \sum_{i=1}^{N} e_{vi}^{T} \left[E_{pi}^{T} g e_{z} - \frac{1}{m_{i}} u_{i0} - \frac{1}{m_{i}} E_{pi}^{T} F_{i} (R_{i} - R_{di}) e_{z} + \frac{1}{m_{i}} E_{pi}^{T} \gamma_{1i} + \dot{E}_{pi}^{T} v_{i} - \dot{\alpha}_{pi} \right],$$
(23)

in which we denote $u_{i0} = E_{pi}^{T} u_{i} \in \mathbb{R}^{3}$, $u_{i} = F_{i} R_{di} e_{z} \in \mathbb{R}^{3}$, and

$$\dot{\alpha}_{pi} = \frac{\partial \alpha_{pi}}{\partial s_i} \dot{s}_i + \frac{\partial \alpha_{pi}}{\partial (p_i - p_{di})} v_i + \sum_{j \in \mathcal{N}_i} \left[\frac{\partial \alpha_{pi}}{\partial (p_i - p_j)} (v_i - v_j) + \frac{\partial \alpha_{pi}}{\partial s_j} \dot{s}_j \right], \tag{24}$$

where $\frac{\partial \alpha_{pi}}{\partial s_i}$ and $\frac{\partial \alpha_{pi}}{\partial s_j}$ are given in Appendix A (see (52) and (53)). Moreover, $\dot{E}_{ni}^{\mathrm{T}} v_i$ in (23) can be expressed as

$$\dot{E}_{pi}^{T} v_{i} = \xi_{ei}^{T} \left(v_{i} - \frac{\mathrm{d}p_{di}}{\mathrm{d}s_{i}} \dot{s}_{i} \right) + \sum_{i \in \mathcal{N}_{i}} \xi_{dij}^{T} (v_{i} - v_{j}), \tag{25}$$

where

$$\begin{aligned} \xi_{ei} &= [Q_{ei}^{\mathsf{T}} v_i, \ 0_3, \ 0_3] \in \mathbb{R}^{3 \times 3}, \\ \xi_{dij} &= [0_3, \ Q_{dij}^{\mathsf{T}} v_i, \ 0_3] \in \mathbb{R}^{3 \times 3}, \end{aligned}$$

where
$$0_3 = [0, 0, 0]^T \in \mathbb{R}^3$$
, $Q_{ei} = \frac{d_{ei}I_3 - (p_i - p_{di})E_{ei}^T}{d_{ei}^2} \in \mathbb{R}^{3 \times 3}$, and $Q_{dij} = \frac{d_{ij}I_3 - (p_i - p_j)E_{dij}^T}{d_{ij}^2} \in \mathbb{R}^{3 \times 3}$, $i = 1, \dots, N, j \in \mathcal{N}_i$.

For ξ_{dij} $(j \in \mathcal{N}_i)$, the $(1 + I_{ij})$ th column vector is $Q_{dij}^{\mathrm{T}} v_i$ and other columns are zero vectors, where I_{ij} is the index of j in the set of neighbors of agent i.

Remark 10: In (25), singularity in Q_{ei} and Q_{dij} can only happen when $d_{ei}=0$ or $d_{ij}=0,\ i,=1,\cdots,N,\ j\in\mathcal{N}_i$. However, in view of the performance and safety constraint requirements (12) and (13), we have $d_{ei}>\varepsilon_{ei}>0$ and $d_{ij}>0$, hence $d_{ei}=0$ and $d_{ij}=0$ will not happen if (12) and (13) are satisfied. Therefore, singularity will not occur in (25).

Now, for the *i*th quadrotor $(i = 1, \dots, N)$, the control law $u_i \in \mathbb{R}^3$ is designed as

$$u_{i} = E_{pi} (E_{pi}^{T} E_{pi})^{-1} u_{i0}, \quad u_{i0} = \hat{m}_{i} \bar{u}_{i0},$$
(26)

$$\bar{u}_{i0} = \Lambda_{pi} \Pi_{pi} + E_{pi}^{T} g e_{z} + K_{vi} e_{vi} + \left(\xi_{ei}^{T} - \frac{\partial \alpha_{pi}}{\partial (p_{i} - p_{di})} \right) v_{i}$$

$$+ \sum_{j \in \mathcal{N}_{i}} \left[\left(\xi_{dij}^{T} - \frac{\partial \alpha_{pi}}{\partial (p_{i} - p_{j})} \right) (v_{i} - v_{j}) - \frac{\partial \alpha_{pi}}{\partial s_{j}} v_{dj} \right]$$

$$- \left(\frac{\partial \alpha_{pi}}{\partial s_{i}} + \xi_{ei}^{T} \frac{d p_{di}}{d s_{i}} \right) v_{di} + \hat{\mu}_{mi} \frac{E_{pi}^{T} E_{pi} e_{vi}}{\sqrt{e_{vi}^{T} E_{pi}^{T} E_{pi} e_{vi} + \varepsilon_{i}^{2}}},$$
(27)

where $K_{vi} > 0$ is a control gain, $\varepsilon_i > 0$ is a design constant, \hat{m}_i is the estimation of the <u>unknown</u> constant m_i , and $\hat{\mu}_{mi}$ is the estimation of the <u>unknown</u> constant μ_{mi} satisfying $\left| \left| -\frac{1}{m} F_i(R_i - R_{di}) e_z + \frac{1}{m} \gamma_{1i} \right| \right| \le \mu_{mi}$.

 $\left| \left| -\frac{1}{m_i} F_i(R_i - R_{\text{d}i}) e_z + \frac{1}{m_i} \gamma_{1i} \right| \right| \leq \mu_{mi}.$ Remark 11: According to the definition of E_{pi} in (20), rank $(E_{pi}) = 3$ under Assumption 1. Therefore $E_{pi}^T E_{pi}$ in (26) is invertible.

Next, we substitute the control design (26) back into (23), which yields

$$-\frac{1}{m_i}e_{vi}^{\mathrm{T}}u_{i0} = -\frac{\hat{m}_i}{m_i}e_{vi}^{\mathrm{T}}\bar{u}_{i0} = -e_{vi}^{\mathrm{T}}\bar{u}_{i0} - \frac{\tilde{m}_i}{m_i}e_{vi}^{\mathrm{T}}\bar{u}_{i0}, \quad (28)$$

where $\tilde{m}_i = \hat{m}_i - m_i$ $(i = 1, \dots, N)$. Hence, (22) and (23) lead to

$$\dot{V}_{1} + \dot{V}_{2}
< \sum_{i=1}^{N} \left(\Pi_{pi}^{T} \Lambda_{pi} e_{vi} - K_{ei} \eta_{ei}^{2} - \sum_{j \in \mathcal{N}_{i}} K_{ij} \eta_{ij}^{2} + \Pi_{pi}^{T} g_{si} z_{si} \right)
- e_{vi}^{T} \bar{u}_{i0} + e_{vi}^{T} E_{pi}^{T} g e_{z} - \frac{\tilde{m}_{i}}{m_{i}} e_{vi}^{T} \bar{u}_{i0} + \frac{1}{m_{i}} e_{vi}^{T} E_{pi}^{T} \gamma_{1i}
- e_{vi}^{T} \dot{\alpha}_{pi} - \frac{1}{m_{i}} e_{vi}^{T} E_{pi}^{T} F_{i} (R_{i} - R_{di}) e_{z} \right).$$
(29)

Note also that in (29), under Assumption 4 we have

$$-\frac{1}{m_{i}}e_{vi}^{T}E_{pi}^{T}F_{i}(R_{i}-R_{di})e_{z}+\frac{1}{m_{i}}e_{vi}^{T}E_{pi}^{T}\gamma_{1i}$$

$$\leq ||E_{pi}e_{vi}|| \left|\left|-\frac{1}{m_{i}}F_{i}(R_{i}-R_{di})e_{z}+\frac{1}{m_{i}}\gamma_{1i}\right|\right|$$

$$<\varepsilon_{i}\mu_{mi}+\mu_{mi}\frac{e_{vi}^{T}E_{pi}^{T}E_{pi}e_{vi}}{\sqrt{e_{vi}^{T}E_{pi}^{T}E_{pi}e_{vi}+\varepsilon_{i}^{2}}}.$$
(30)

Therefore, it follows from (29) that

$$\begin{aligned}
\dot{V}_{1} + \dot{V}_{2} \\
< \sum_{i=1}^{N} \left[-K_{ei} \eta_{ei}^{2} - \sum_{j \in \mathcal{N}_{i}} K_{ij} \eta_{ij}^{2} - K_{vi} e_{vi}^{\mathsf{T}} e_{vi} \right. \\
&+ \left(\Pi_{pi}^{\mathsf{T}} g_{si} - e_{vi}^{\mathsf{T}} \xi_{ei}^{\mathsf{T}} \frac{\mathrm{d} p_{di}}{\mathrm{d} s_{i}} - e_{vi}^{\mathsf{T}} \frac{\partial \alpha_{pi}}{\partial s_{i}} \right) z_{si} - \frac{\tilde{m}_{i}}{m_{i}} e_{vi}^{\mathsf{T}} \bar{u}_{i} \\
&- \tilde{\mu}_{mi} \frac{e_{vi}^{\mathsf{T}} E_{pi}^{\mathsf{T}} E_{pi} e_{vi}}{\sqrt{e_{vi}^{\mathsf{T}} E_{pi}^{\mathsf{T}} E_{pi} e_{vi} + \varepsilon_{i}^{2}} + \varepsilon_{i} \mu_{mi} \right],
\end{aligned} (31)$$

where $\tilde{\mu}_{mi} = \hat{\mu}_{mi} - \mu_{mi}$ $(i = 1, \dots, N)$.

Next, design the adaptive laws for the estimators \hat{m}_i and $\hat{\mu}_{mi}$, and the path parameter timing law \ddot{s}_i of the *i*th quadrotor $(i = 1, \dots, N)$ as the following

$$\dot{\hat{m}}_i = n_{mi} e_{vi}^{\mathrm{T}} \bar{u}_{i0} - \sigma_{mi} \hat{m}_i, \tag{32}$$

$$\dot{\hat{\mu}}_{mi} = n_{\mu mi} \frac{e_{vi}^{T} E_{pi}^{T} E_{pi} e_{vi}}{\sqrt{e_{vi}^{T} E_{pi}^{T} E_{pi} e_{vi} + \varepsilon_{i}^{2}}} - \sigma_{\mu mi} \hat{\mu}_{mi}, \tag{33}$$

$$\ddot{s}_{i} = e_{vi}^{\mathsf{T}} \xi_{ei}^{\mathsf{T}} \frac{\mathrm{d}p_{\mathrm{d}i}}{\mathrm{d}s_{i}} + e_{vi}^{\mathsf{T}} \frac{\partial \alpha_{pi}}{\partial s_{i}} - \Pi_{pi}^{\mathsf{T}} g_{si} + \sum_{j \in \mathcal{N}_{i}} e_{vj}^{\mathsf{T}} \frac{\partial \alpha_{pi}}{\partial s_{j}} - K_{si} z_{si} + \frac{\mathrm{d}v_{\mathrm{d}i}}{\mathrm{d}s_{i}} \dot{s}_{i},$$
(34)

where $\hat{m}_i(0) = \hat{m}_{i0}$, $\hat{\mu}_{mi}(0) = \hat{\mu}_{mi0}$, $s_i(0) = s_{i10}$, and $\dot{s}_i(0) = s_{i20}$. n_{mi} , $n_{\mu mi}$, σ_{mi} , $\sigma_{\mu mi}$, and K_{si} are positive design constants. Let $V_m = \sum_{i=1}^N \frac{1}{2n_{mi}m_i} \tilde{m}_i^2$, $V_{\mu m} = \sum_{i=1}^N \frac{1}{2n_{\mu mi}} \tilde{\mu}_{mi}^2$, $V_s = \sum_{i=1}^N \frac{1}{2} z_{si}^2$. Denote $V_{pos} = V_1 + V_2 + V_m + V_{\mu m} + V_s$,

for its time derivative we can get

$$\dot{V}_{\text{pos}} < \sum_{i=1}^{N} \left(-K_{\text{e}i} \eta_{\text{e}i}^{2} - \sum_{j \in \mathcal{N}_{i}} K_{ij} \eta_{ij}^{2} - K_{vi} e_{vi}^{\text{T}} e_{vi} - K_{si} z_{si}^{2} \right. \\
\left. - \frac{\sigma_{mi}}{2n_{mi} m_{i}} \tilde{m}_{i}^{2} - \frac{\sigma_{\mu mi}}{2n_{\mu mi}} \tilde{\mu}_{mi}^{2} + C_{1i} \right), \tag{35}$$

where $C_{1i} = \frac{\sigma_{mi}}{2n_{mi}}m_i + \frac{\sigma_{\mu mi}}{2n_{\mu mi}}\mu_{mi}^2 + \varepsilon_i\mu_{mi}$. Hence,

$$\dot{V}_{\text{pos}} < -\kappa_1 V_{\text{pos}} + \varrho_1, \tag{36}$$

where $\kappa_1 \triangleq \min_{i,j} (2K_{ei}, 2K_{ij}, 2K_{vi}, 2K_{si}, \sigma_{mi}, \sigma_{\mu mi}), \ \varrho_1 \triangleq \sum_{i=1}^{N} C_{1i}$. The aforementioned design procedure leads to the following theoretical result.

Theorem 1: For the *i*th quadrotor ($i = 1, \dots, N$), with the thrust law as (26) and (27), adaptive laws (32) and (33), and the path parameter timing law (34), the quadrotor formation system described by (1) and (4), under Assumptions 1-6 will have the following results:

- 1) The path-dependent constraint requirements (12) and (13) will be met during formation.
- 2) The transformed output tracking errors η_{ei} and η_{ij} ($i = 1, \dots, N, j \in \mathcal{N}_i$) will converge into the set

$$\left\{ x = \eta_{ei}, \eta_{ij} : |x| < \varepsilon_{\eta}, \quad \varepsilon_{\eta} = \sqrt{\frac{2\varrho_{1}}{\kappa_{1}}} \right\}, \quad (37)$$

which implies that the output tracking errors d_{ei} and d_{eij} will converge into the following regions

$$\left\{ d_{ei} : \max(\varepsilon_{ei}, 2\varepsilon_{ei} + \varepsilon_{\chi_{Li}}) < d_{ei} < 2\varepsilon_{ei} + \varepsilon_{\chi_{Hi}} \right\}, \tag{38}$$

$$\left\{ d_{eij} : -\varepsilon_{\iota_{\text{L}ij}} < d_{eij} < \varepsilon_{\iota_{\text{H}ij}} \right\},$$
 (39)

where $\varepsilon_{\chi_{\mathrm{H}i}}$ and $\varepsilon_{\chi_{\mathrm{L}i}}$ are expressed as

$$\varepsilon_{\chi_{\mathrm{H}i}} = \frac{ \left\{ \begin{split} & \left[\varepsilon_{\eta} (\Omega_{d\mathrm{H}i} - \varepsilon_{ei}) - \Omega_{d\mathrm{H}i} \right] \\ & + \sqrt{ \left[\varepsilon_{\eta} (\Omega_{d\mathrm{H}i} - \varepsilon_{ei}) - \Omega_{d\mathrm{H}i} \right]^2 \\ & + 4 \varepsilon_{\eta}^2 \Omega_{d\mathrm{H}i} \varepsilon_{ei} \end{split} \right\} }{2 \varepsilon_{\eta}}, \\ & \left\{ \begin{split} & \left[\varepsilon_{\eta} (\Omega_{d\mathrm{H}i} - \varepsilon_{ei}) - \Omega_{d\mathrm{H}i} \right] \\ & - \sqrt{ \left[\varepsilon_{\eta} (\Omega_{d\mathrm{H}i} - \varepsilon_{ei}) + \Omega_{d\mathrm{H}i} \right]^2 \\ & + 4 \varepsilon_{\eta}^2 \Omega_{d\mathrm{H}i} \varepsilon_{ei}} \end{split} \right\} }{2 \varepsilon_{\eta}}. \end{split}$$

Moreover, $\varepsilon_{l_{\text{H}ij}}$ and $\varepsilon_{l_{\text{L}ij}}$ can be written as

$$\varepsilon_{t_{\mathrm{H}ij}} = \frac{\begin{pmatrix} -[\Omega_{\mathrm{H}ij}\Omega_{\mathrm{L}ij} - \varepsilon_{\eta}(\Omega_{\mathrm{H}ij} - \Omega_{\mathrm{L}ij})] \\ + \sqrt{\Omega_{\mathrm{H}ij}^2\Omega_{\mathrm{L}ij}^2 + \varepsilon_{\eta}^2(\Omega_{\mathrm{H}ij} + \Omega_{\mathrm{L}ij})^2} \\ + \sqrt{\Omega_{\mathrm{H}ij}^2\Omega_{\mathrm{L}ij}^2 + \varepsilon_{\eta}^2(\Omega_{\mathrm{H}ij} - \Omega_{\mathrm{L}ij})} \\ 2\varepsilon_{\eta} \\ \\ \varepsilon_{t_{\mathrm{L}ij}} = \frac{\begin{pmatrix} -[\Omega_{\mathrm{H}ij}\Omega_{\mathrm{L}ij} + \varepsilon_{\eta}(\Omega_{\mathrm{H}ij} - \Omega_{\mathrm{L}ij})] \\ + \sqrt{\Omega_{\mathrm{H}ij}^2\Omega_{\mathrm{L}ij}^2 + \varepsilon_{\eta}^2(\Omega_{\mathrm{H}ij} + \Omega_{\mathrm{L}ij})^2} \\ + 2\varepsilon_{\eta}\Omega_{\mathrm{H}ij}\Omega_{\mathrm{L}ij}(\Omega_{\mathrm{H}ij} - \Omega_{\mathrm{L}ij}) \end{pmatrix}} \\ & \frac{2\varepsilon_{\eta}}{2\varepsilon_{\eta}} \\ -\frac{2\varepsilon_{\eta}}{2\varepsilon_{\eta}} \\ -\frac{2\varepsilon_{\eta}}{2$$

3) The *i*th quadrotor's desired speed assignment along the path $v_{\mathrm{d}i}$ ($i=1,\cdots,N$) can be satisfied, i.e., $\limsup_{t\to\infty} |\dot{s}_i - v_{\mathrm{d}i}| < \varepsilon_{\eta}$.

4) The adaptive laws (32) and (33), and the path parameter timing laws (34), are all uniformly bounded.

Proof: From (36) we have

$$V_{\text{pos}}(t) < \left(V_{\text{pos}}(0) - \frac{\varrho_1}{\kappa_1}\right)e^{-\kappa_1 t} + \frac{\varrho_1}{\kappa_1}.$$
 (40)

The uniform boundedness of V_{pos} in turn implies boundedness of η_{ei} and η_{ij} ($i=1,\cdots,N,\ j\in\mathcal{N}_i$). Hence, the constraints requirements (12) and (13) are both satisfied during the operation.

Moreover, we have $\limsup_{t\to\infty} V_{\text{pos}} < \frac{\varrho_1}{\kappa_1}$, hence $\frac{1}{2}\eta_{ei}^2 < \frac{\varrho_1}{\kappa_1}$ when $t\to\infty$, therefore η_{ei} will converge to the set (37). Similar relationship holds for η_{ij} . Furthermore, uniform boundedness of V_{pos} implies boundedness of the adaptive estimates \hat{m}_i and $\hat{\mu}_{mi}$, as well as boundedness of fictitious errors e_{vi} $(i=1,\cdots,N)$.

Next, note that in the range $-\varepsilon_{ei} < d_{\varepsilon ei} < \Omega_{dHi}$, η_{ei} is a function in $d_{\varepsilon ei}$. Recall that $d_{\varepsilon ei} \triangleq d_{ei} - 2\varepsilon_{ei}$, with $\varepsilon_{ei} > 0$ being an arbitrarily small constant. Hence, the range (12) gives the range for d_{ei} given in (38). Besides, within the range of (13), η_{ij} is quadratically related to d_{eij} . Hence, satisfying the constraints (12) and (13) means that the distance tracking errors d_{ei} and d_{eij} will be confined in the ranges defined by (38) and (39).

Furthermore, since $\limsup_{t\to\infty}\frac{1}{2}z_{si}^2<\frac{\varrho_1}{\kappa_1}$, the speed assignment errors will satisfy $|\dot{s}_i-v_{\mathrm{d}i}|<\varepsilon_\eta$ when $t\to\infty$. Besides, the boundedness of $v_{\mathrm{d}i}$ will lead to the boundedness of \dot{s}_i .

Finally, for the ith qudrotor, boundedness of the adaptive estimates \hat{m}_i and $\hat{\mu}_{mi}$, the path parameter speed \dot{s}_i , and the fictitious error e_{vi} as well as the invertibility of $E_{pi}^T E_{pi}$ can be utilized to check that α_{pi} , u_i , u_{i0} , and \bar{u}_{i0} are all uniformly bounded. Hence, it is clear to imply that the adaptive laws (32) and (33), and the path parameter timing law (34), are all uniformly bounded.

Remark 12: In Theorem 1, using L'Hôpital's rule we can derive that

$$\lim_{\varepsilon_n \to 0} \varepsilon_{\chi_{\text{H}i}}, \ \varepsilon_{\chi_{\text{L}i}}, \ \varepsilon_{\ell_{\text{H}ij}}, \ \varepsilon_{\ell_{\text{L}ij}} = 0, \tag{41}$$

for $i=1,\cdots,N, j\in\mathcal{N}_i$. This implies that when the modified error variables η_{ei} and η_{ij} converge into small neighborhoods of zero, the relative distance tracking error d_{eij} will converge to a region close to zero and the distance tracking error d_{ei} will converge to a region arbitrarily close to $2\varepsilon_{ei}$, with $\varepsilon_{ei} > 0$ being an arbitrarily small constant.

Remark 13: To reduce the size of the set in (37), we need to select large κ_1 and small ϱ_1 . To make κ_1 large, we can select large control gains K_{ei} , K_{ij} , and K_{vi} , for $i=1,\cdots,N$, $j \in \mathcal{N}_i$ and large adaptive and path timing control parameters σ_{mi} , $\sigma_{\mu mi}$, and K_{si} . To make ϱ_1 small, we can select small ε_i , and large adaptive control parameters n_{mi} and $n_{\mu mi}$.

B. Attitude Control Design and Results

Sten 3

Next, we address the attitude kinematics of the quadrotors. Let $V_3 = \sum_{i=1}^N \frac{1}{2} e_{\Theta i}^T e_{\Theta i}$. With some algebraic analysis shown in Appendix B (see (54)-(59)), the stabilizing function $\alpha_{\Theta i} \in$

 \mathbb{R}^3 for the *i*th quadrotor $(i = 1, \dots, N)$ is designed as

$$\alpha_{\Theta i} = -(K_{\Theta i} + \nu_i) T_i^{-1} e_{\Theta i}, \tag{42}$$

where $K_{\Theta i} > 0$ is a control gain and $\nu_i > 0$ is a design constant.

Step 4:

At this step, let $V_4 = \sum_{i=1}^{N} \frac{1}{2} e_{\omega i}^{\mathrm{T}} e_{\omega i}$. With some algebraic analysis shown in Appendix C (see (60)-(65)), the torque law and adaptive laws for the *i*th quadrotor $(i = 1, \dots, N)$ are designed as

$$\tau_i = -\frac{e_{\omega i} \bar{\tau}_i^{\mathrm{T}} \bar{\tau}_i \hat{\rho}_{Ji}^2}{\sqrt{e_{\omega i}^{\mathrm{T}} e_{\omega i} \bar{\tau}_i^{\mathrm{T}} \bar{\tau}_i \hat{\rho}_{Ji}^2 + \varepsilon_i^2}},\tag{43}$$

$$\bar{\tau}_{i} = (K_{\Theta i} + \nu_{i}) \left(\frac{\mathrm{d}(T_{i}^{-1})}{\mathrm{d}t} e_{\Theta i} + \omega_{i} \right) + K_{\omega i} e_{\omega i} + T_{i}^{\mathrm{T}} e_{\Theta i}$$

$$+ \hat{\mu}_{J i} \frac{e_{\omega i}}{\sqrt{e_{\omega i}^{\mathrm{T}} e_{\omega i} + \varepsilon_{i}^{2}}} + \hat{h}_{\bar{J} i} \frac{e_{\omega i} \bar{\omega}_{i}^{\mathrm{T}} \bar{\omega}_{i}}{\sqrt{e_{\omega i}^{\mathrm{T}} e_{\omega i} \bar{\omega}_{i}^{\mathrm{T}} \bar{\omega}_{i} + \varepsilon_{i}^{2}}}, \quad (44)$$

$$\dot{\hat{\rho}}_{Ji} = n_{\rho Ji} e_{\omega i}^{\mathsf{T}} \bar{\tau}_i - \sigma_{\rho Ji} \hat{\rho}_{Ji}, \tag{45}$$

$$\dot{\hat{h}}_{\bar{J}i} = n_{h\bar{J}i} \frac{e_{\omega i}^{\mathrm{T}} e_{\omega i} \bar{\omega}_{i}^{\mathrm{T}} \bar{\omega}_{i}}{\sqrt{e_{\omega i}^{\mathrm{T}} e_{\omega i} \bar{\omega}_{i}^{\mathrm{T}} \bar{\omega}_{i} + \varepsilon_{i}^{2}}} - \sigma_{h\bar{J}i} \hat{h}_{\bar{J}i}, \tag{46}$$

$$\dot{\hat{\mu}}_{Ji} = n_{\mu Ji} \frac{e_{\omega i}^{\mathsf{T}} e_{\omega i}}{\sqrt{e_{\omega i}^{\mathsf{T}} e_{\omega i} + \varepsilon_{i}^{2}}} - \sigma_{\mu Ji} \hat{\mu}_{Ji}, \tag{47}$$

where $\hat{\rho}_{Ji}(0) = \hat{\rho}_{Ji0}$, $\hat{h}_{\bar{J}i}(0) = \hat{h}_{\bar{J}i0}$, and $\hat{\mu}_{Ji}(0) = \hat{\mu}_{Ji0}$ are the initial conditions. $K_{\omega i} > 0$ is a control gain. $\hat{\mu}_{Ji}$ is the estimator of the <u>unknown</u> constant μ_{Ji} expressed in (65), $\hat{h}_{\bar{J}i}$ is the estimator of the <u>unknown</u> constant $\bar{h}_{\bar{J}i}$ expressed in (61), and $\hat{\rho}_{Ji}$ is the estimator of the <u>unknown</u> constant $\rho_{Ji} = \frac{1}{b_{Ji}}$. $n_{\rho Ji}$, $\sigma_{\rho Ji}$, $n_{h\bar{J}i}$, $\sigma_{h\bar{J}i}$, $n_{\mu Ji}$, and $\sigma_{\mu Ji}$ are positive design constants

Now, let $V_{\rho J} = \sum_{i=1}^{N} \frac{\underline{b}_{Ji}}{2n_{\rho Ji}} \tilde{\rho}_{Ji}^2$, $V_{h\bar{J}} = \sum_{i=1}^{N} \frac{1}{2n_{h\bar{J}i}} \tilde{h}_{\bar{J}i}^2$, $V_{\mu J} = \sum_{i=1}^{N} \frac{1}{2n_{\mu Ji}} \tilde{\mu}_{Ji}^2$. Denote $V_{\rm att} = V_3 + V_4 + V_{\rho J} + V_{h\bar{J}} + V_{\mu J}$, after some algebraic manipulation, we can arrive at

$$\dot{V}_{\text{att}} < \sum_{i=1}^{N} \left(-K_{\Theta i} e_{\Theta i}^{\text{T}} e_{\Theta i} - K_{\omega i} e_{\omega i}^{\text{T}} e_{\omega i} - \frac{\underline{b}_{Ji} \sigma_{\rho Ji}}{2n_{\rho Ji}} \tilde{\rho}_{Ji}^{2} - \frac{\sigma_{h \bar{J}i}}{2n_{\nu Ji}} \tilde{h}_{\bar{J}i}^{2} - \frac{\sigma_{\mu Ji}}{2n_{\nu Ji}} \tilde{\mu}_{Ji}^{2} + C_{2i} \right),$$
(48)

where $C_{2i} = \varepsilon_i (\bar{h}_{\bar{J}i} + \mu_{Ji} + \underline{b}_{Ji}) + \frac{\underline{b}_{Ji}\sigma_{\rho Ji}}{2n_{\rho Ji}} \rho_{Ji}^2 + \frac{\sigma_{h\bar{J}i}}{2n_{h\bar{J}i}} \bar{h}_{\bar{J}i}^2 + \frac{\sigma_{\mu Ji}}{2n_{\mu Ji}} \mu_{Ji}^2 + \frac{1}{\nu_i} \bar{\Theta}_{di}^2$. Hence, we can get

$$\dot{V}_{\text{att}} < -\kappa_2 V_{\text{att}} + \rho_2, \tag{49}$$

where $\kappa_2 \triangleq \min_i (2K_{\Theta i}, 2K_{\omega i}, \sigma_{\rho J i}, \sigma_{h \bar{J} i}, \sigma_{\mu J i}), \quad \varrho_2 \triangleq \sum_{i=1}^{N} C_{2i}$. The above backstepping design for the attitude leads to the following theorem.

The overall control algorithm can be summarized into the block diagram in Figure 3.

Theorem 2: For the *i*th quadrotor $(i = 1, \dots, N)$, with the torque law as (43) and (44), and adaptive laws (45), (46), and (47), the quadrotor formation system described by (2) and (5), under Assumptions 1–6, achieves the following performance:

1) The attitude tracking error $e_{\Theta i}$ $(i = 1, \dots, N)$ will converge into the sets

$$\left\{ x = e_{\phi i}, e_{\theta i}, e_{\psi i} : |x| < \varepsilon_{\eta}, \quad \varepsilon_{\eta} = \sqrt{\frac{2\varrho_2}{\kappa_2}} \right\}, \quad (50)$$

2) The control torque laws (43) and (44), and adaptive laws (45), (46), and (47), are all uniformly bounded.

Proof: Following (49), we can conclude that the Lyapunov function $V_{\rm att}$ is bounded, since from (49) we can get

$$V_{\text{att}}(t) < \left(V_{\text{att}}(0) - \frac{\varrho_2}{\kappa_2}\right)e^{-\kappa_2 t} + \frac{\varrho_2}{\kappa_2}.$$
 (51)

The uniform boundedness of $V_{\rm att}$ in turn implies boundedness of $e_{\phi i}$, $e_{\theta i}$, and $e_{\psi i}$ ($i=1,\cdots,N$). Moreover, we have $\limsup_{t\to\infty}V_{\rm att}<\frac{\varrho_2}{\kappa_2}$, hence $\frac{1}{2}e_{\phi i}^2<\frac{\varrho_2}{\kappa_2}$ when $t\to\infty$, therefore $e_{\phi i}$ will converge to the set (50). Similar relationships hold for $e_{\theta i}$ and $e_{\psi i}$. The boundedness of adaptive estimates $\hat{\rho}_{Ji}$, $\hat{h}_{\bar{J}i}$, and $\hat{\mu}_{Ji}$, as well as boundedness of fictitious errors $e_{\omega i}$, can be concluded from the fact that $V_{\rm att}$ is bounded. This implies that the torque law (43) and (44), and adaptive laws (45), (46), and (47), are all bounded.

V. SIMULATION STUDIES

We conduct a simulation with a team of N = 4quadrotors. For i = 1, 2, 3, 4, the model parameters of the quadrotors are $m_i = 4$ kg, g = 9.81m/s², $J_i = \text{diag}(0.109, 0.103, 0.0625)$ kg·m². Note that the units of the position, attitude, translational and angular velocities are m, rad, m/s, and rad/s, respectively. The communication topology for the UAV team is selected as $\mathcal{N}_1 = \{2,3\}, \ \mathcal{N}_2 = \{1,4\}, \ \mathcal{N}_3 = \{1,4\}, \ \text{and}$ $\mathcal{N}_4 = \{2, 3\}$. The desired paths for vehicles are given as $p_{d1}(s_1) = \begin{bmatrix} 0.6\cos(0.7s_1) + 0.015s_1, & 0.6\sin(0.7s_1) \end{bmatrix}$ $+ 0.015s_1, -0.4s_1 - 0.3$ ^T, $p_{d2}(s_2) = [0.6\cos(0.7s_2) +$ $0.015s_2$, $2.15 + 0.6\sin(0.7s_2) + 0.015s_2$, $-0.4s_2 - 0.6$, $p_{d3}(s_3) = [2 + 0.6\cos(0.7s_3), 0.6\sin(0.7s_3), -0.4s_3 [0.4]^{\mathrm{T}}$, and $p_{\mathrm{d4}}(s_4) = [1.0 + 0.6\cos(0.7s_4), 1.0 + 0.6\cos(0.7s_4)]$ $0.6\sin(0.7s_4)$, $-0.4s_4 - 1$ with reference yaw signal $\psi_{di} = 0$, i = 1, 2, 3, 4, and the desired speed assignment is $v_{di} = \left| \frac{dp_{di}}{ds_i} \right|$. The constraint functions are selected as $\Omega_{\text{H}i}(s_i) \stackrel{\text{i.i.}}{=} (3.0 - 0.25)e^{-1.1s_i} + 0.25$, $\Omega_{\text{H}ij}(s_i, s_j) = (1.5 - 0.1)\frac{e^{-0.4s_i} + e^{-0.4s_j}}{2} + 0.1$, and $\Omega_{\text{L}ij}(s_i, s_j) = (0.7 - 0.25)e^{-0.2s_i} = (0.7 - 0.25)e^{-0.2s_i}$ $(0.1)\frac{e^{-0.2s_i}+e^{-0.2s_j}}{2} + 0.1, i = 1, 2, 3, 4, j \in \mathcal{N}_i$. The lower bounds for the distance tracking errors are chosen as ε_{ei} = 0.005, i = 1, 2, 3, 4.

Next, the design parameters are chosen as $\varepsilon_i = 0.1$, $n_{mi} = 1.59$, $n_{\mu mi} = 2.0$, $n_{\rho Ji} = 0.6$, $n_{h\bar{J}i} = 0.6$, $n_{\mu Ji} = 0.2$, $\sigma_{mi} = 0.1$, $\sigma_{\mu mi} = 0.1$, $\sigma_{\rho Ji} = 0.01$, $\sigma_{h\bar{J}i} = 0.01$, $\sigma_{\mu Ji} = 0.01$, and $K_s = 50$, i = 1, 2, 3, 4. The control gains are designed as $K_{ei} = 0.8$, $K_{ij} = 0.55$, $K_{vi} = 5$, $v_i = 0.5$, $K_{\Theta i} = 2$, and $K_{\omega i} = 4$, i = 1, 2, 3, 4, $j \in \mathcal{N}_i$. The initial positions of the quadrotor team are $p_1(0) = [0.25, 0, 1]^T$, $p_2(0) = [0, 2, 1.5]^T$, $p_3(0) = [2, 0, 1.2]^T$, and $p_4(0) = [2, 2, 1.0]^T$. The initial attitudes of quadrotors are $\Theta_i(0) = [0, 0, 0.1]^T$, i = 1, 2, 3, 4. The initial conditions of translational and angular velocities of every agent are zero. The external disturbances

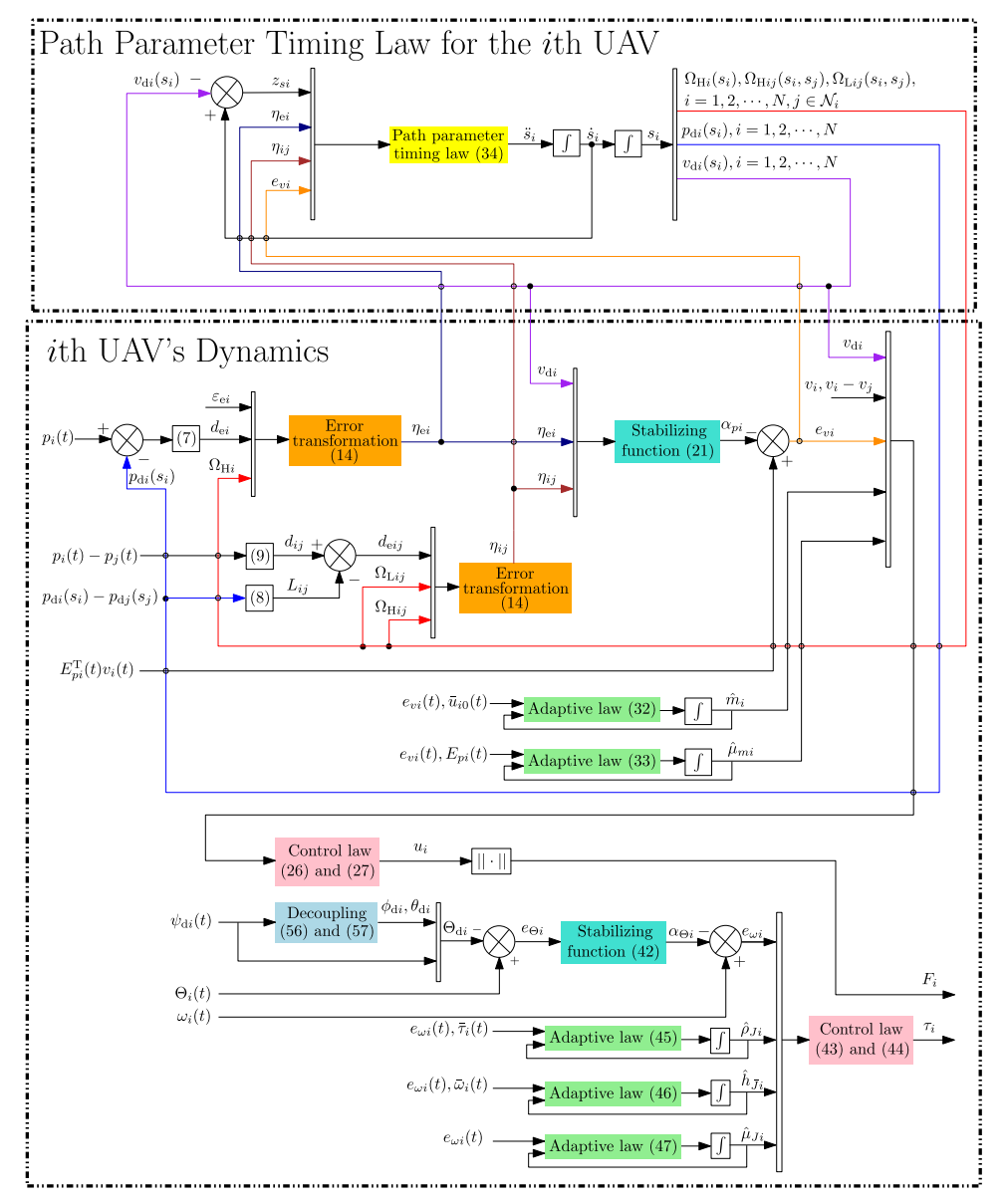


Fig. 3. Block diagram of the overall control algorithm.

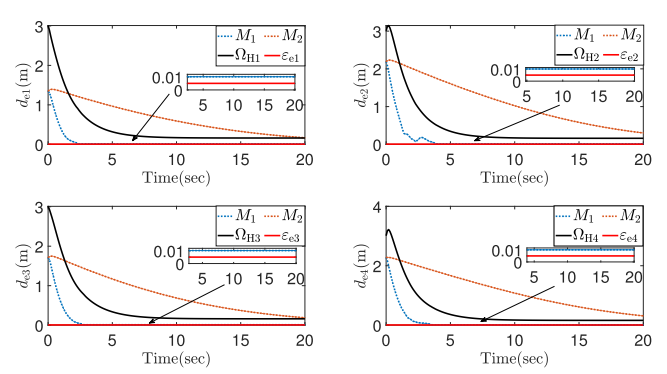


Fig. 4. The profile of distance tracking errors d_{ei} under the proposed controller (M_1) and trajectory-tracking formation controller (M_2) [48] with $\varepsilon_{ei}>0$ and path-dependent constraint functions $\Omega_{d{\rm H}i}$.

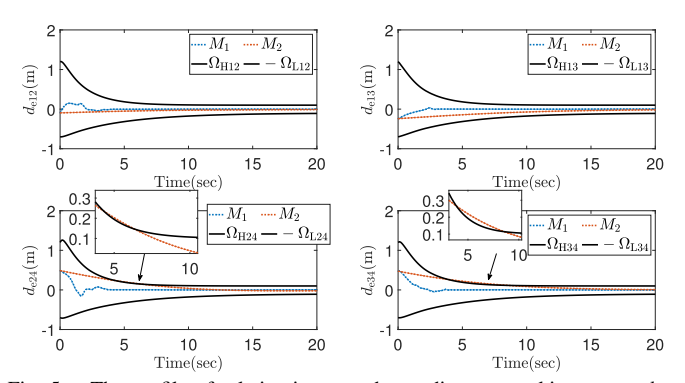


Fig. 5. The profile of relative inter-quadrotor distance tracking errors d_{eij} under the proposed controller (M_1) and the trajectory-tracking formation controller (M_2) [48] with constraint functions $\Omega_{{\rm H}ij}$ and $\Omega_{{\rm L}ij}$.

are $\gamma_{1i} = \begin{bmatrix} 0.11 \sin(0.2t), & 0.06 \cos(0.15t), & 0.03 \cos(0.12t) \end{bmatrix}^{T}$ and $\gamma_{2i} = \begin{bmatrix} 0.03 \sin(0.25t), & 0.04 \sin(0.2t), & 0.06 \cos(0.3t) \end{bmatrix}^{T}$, where i = 1, 2, 3, 4.

In order to show the effectiveness of our proposed control framework, we conduct a comparative study with a trajectory-tracking formation controller [48] which does not account for path-dependent constraint requirements. In [48],

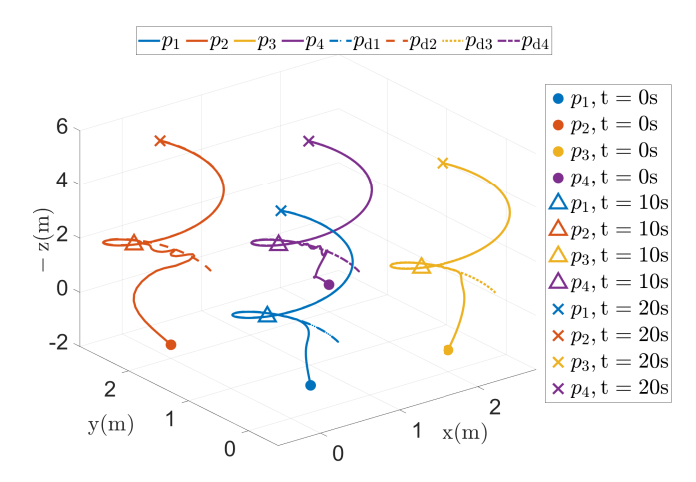


Fig. 6. Trajectories of the quadrotors in 3D space.

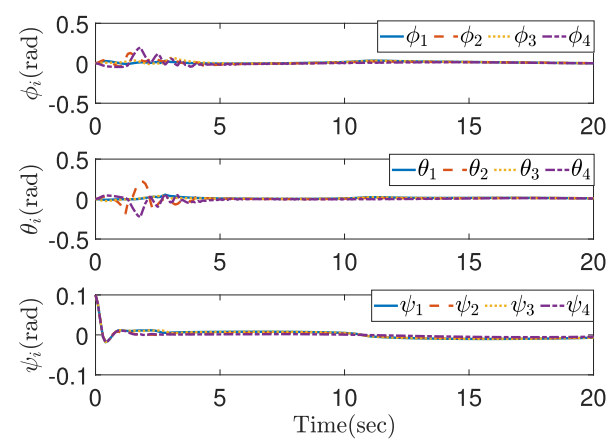


Fig. 7. The profile of quadrotors' attitude ϕ_i , θ_i , and ψ_i .

control gains and design parameters are $K_p = 0.8$, $K_v = 5$, $K_a = 50$, and $K_q = 16$. The model parameters of quadrotors are selected the same as in our simulation. Moreover, both controllers operate with identical external disturbances and initial states for the UAV team. The simulation results are presented in Figures 4-10. Distance tracking errors d_{ei} under the proposed path-dependent constrained formation controller (M_1) and trajectory-tracking formation controller (M_2) [48] are shown in Figure 4. On the one hand, the performance constraint requirements for all agents under the trajectorytracking formation controller (M_2) [48] are violated when $t \ge$ 3. On the other hand, under the proposed controller (M_1) , d_{ei} can converge to small regions close to $2\varepsilon_{ei}$ without violating performance constraint requirements, which is not the case with the trajectory-tracking formation controller (M_2) . Next, Figure 5 gives the profile of inter-quadrotor distance tracking errors d_{eij} under the proposed path-dependent constrained formation controller (M_1) and trajectory-tracking formation controller (M_2) [48]. On the one hand, we can observe that safety constraints are never violated during the formation operation when applying the proposed controller (M_1) . On the other hand, under the trajectory-tracking formation controller (M_2) [48], the higher safety constraint requirements Ω_{H24} and $\Omega_{\rm H34}$ for the relative distance tracking errors $d_{\rm e24}$ and $d_{\rm e34}$ are violated when t > 3.

The 3D trajectories of the four quadrotors are depicted in Figure 6. The effectiveness of our proposed formation

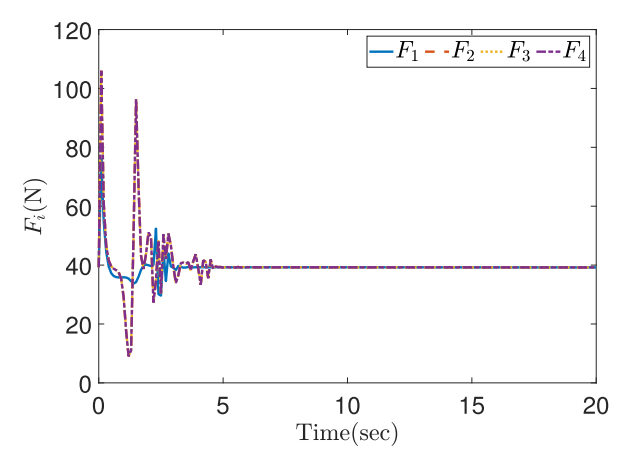


Fig. 8. The profile of quadrotors's thrust F_i .

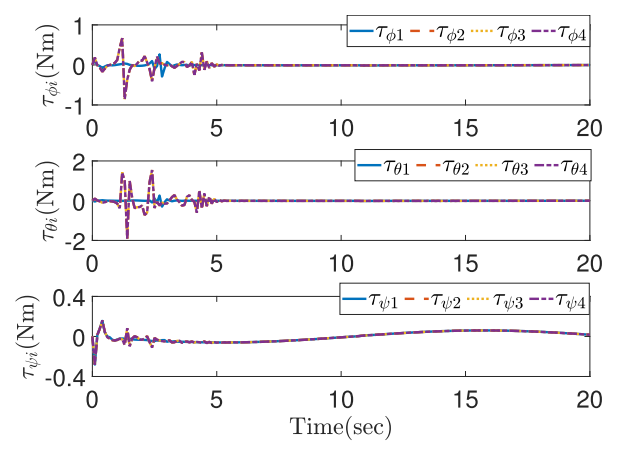


Fig. 9. The profile of quadrotors' torques $\tau_{\phi i}$, $\tau_{\theta i}$, and $\tau_{\psi i}$.

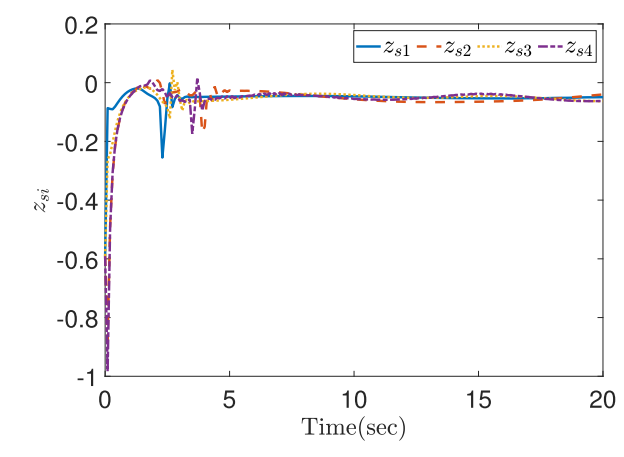


Fig. 10. Path speed errors z_{si} profile.

algorithm is evident in the precise path following of quadrotors over time. The profile of quadrotor attitudes, ϕ_i , θ_i , and ψ_i presented in Figure 7 shows the stabilization of the attitudes despite the lack of model parameters and influence of the external disturbance γ_{2i} .

Moreover, the thrust F_i and torques $\tau_{\phi i}$, $\tau_{\theta i}$, and $\tau_{\psi i}$ are plotted in Figures 8 and 9, respectively. The thrust F_i can converge to a region close to the gravitational force of the quadrotor with system uncertainties and unknown time-varying external disturbances. The torques can accommodate the disturbance γ_{2i} despite the lack of accurate model parameters. Finally, the path speed errors z_{si} are exhibited in

Figure 10, which shows the path speed errors can converge to neighborhoods of the origin. To summarize, the aforementioned simulation results align with the theoretic analysis discussed in Theorems 1 and 2.

VI. CONCLUSION

For the first time in the formation control literature, we propose a new formulation of path-dependent constraints during UAV formation operation. Specifically, we develop a path-dependent constrained formation control framework to address path-dependent performance and safety constraints. Universal barrier functions are incorporated into the controller design and analysis, to ensure that the constraint requirements on the distance tracking errors and relative distance tracking errors are both satisfied during the operation. Under the proposed constrained formation architecture, the distance tracking errors and relative inter-quadrotor distance errors can exponentially converge to small regions near the equilibrium, meanwhile all constraint requirements can be guaranteed. In the future, research directions include path-dependent constrained formation control problems for UAVs with collaborate objectives, such as load lifting and transporting with path-dependent system uncertainties.

APPENDIX A STEP 2 OF BACKSTEPPING DESIGN

$$\frac{\partial \alpha_{pi}}{\partial s_{i}} = -\frac{\partial \alpha_{pi}}{\partial (p_{i} - p_{di})} \frac{dp_{di}}{ds_{i}} + \frac{\partial \alpha_{pi}}{\partial \Omega_{dHi}} \frac{d\Omega_{dHi}}{ds_{i}} + \frac{\partial \alpha_{pi}}{\partial v_{di}} \frac{dv_{di}}{ds_{i}}
+ \frac{\partial \alpha_{pi}}{\partial (\frac{d\Omega_{dHi}}{ds_{i}})} \frac{d^{2}\Omega_{dHi}}{ds_{i}^{2}} + \frac{\partial \alpha_{pi}}{\partial (\frac{dp_{di}}{ds_{i}})} \frac{d^{2}p_{di}}{ds_{i}^{2}}
+ \sum_{j \in \mathcal{N}_{i}} \left[\frac{\partial \alpha_{pi}}{\partial \Omega_{Hij}} \frac{\partial \Omega_{Hij}}{\partial s_{i}} + \frac{\partial \alpha_{pi}}{\partial \Omega_{Lij}} \frac{\partial \Omega_{Lij}}{\partial s_{i}} \right]
+ \frac{\partial \alpha_{pi}}{\partial (\frac{\partial \Omega_{Hij}}{\partial s_{i}})} \frac{\partial^{2}\Omega_{Hij}}{\partial s_{i}^{2}} + \frac{\partial \alpha_{pi}}{\partial (\frac{\partial \Omega_{Lij}}{\partial s_{i}})} \frac{\partial^{2}\Omega_{Lij}}{\partial s_{i}^{2}}
+ \frac{\partial \alpha_{pi}}{\partial (p_{di} - p_{dj})} \frac{dp_{di}}{ds_{i}} \right],$$
(52)
$$\frac{\partial \alpha_{pi}}{\partial s_{j}} = -\frac{\partial \alpha_{pi}}{\partial (p_{di} - p_{dj})} \frac{dp_{dj}}{ds_{j}} + \frac{\partial \alpha_{pi}}{\partial \Omega_{Hij}} \frac{\partial \Omega_{Hij}}{\partial s_{j}}
+ \frac{\partial \alpha_{pi}}{\partial \Omega_{Lij}} \frac{\partial \Omega_{Lij}}{\partial s_{j}} + \frac{\partial \alpha_{pi}}{\partial (\frac{\partial \Omega_{Hij}}{\partial s_{i}})} \frac{\partial^{2}\Omega_{Hij}}{\partial s_{i}\partial s_{j}}
+ \frac{\partial \alpha_{pi}}{\partial \Omega_{Lij}} \frac{\partial^{2}\Omega_{Lij}}{\partial s_{i}\partial s_{j}}.$$
(53)

APPENDIX B STEP 3 OF BACKSTEPPING DESIGN

First, we need to extract the reference attitude from the position control design. Recall that $u_i = F_i R_{di} e_z$, we have

$$u_{i} = F_{i} \begin{bmatrix} c\phi_{di} s\theta_{di} c\psi_{di} + s\phi_{di} s\psi_{di} \\ c\phi_{di} s\theta_{di} s\psi_{di} - s\phi_{di} c\psi_{di} \\ c\phi_{di} c\theta_{di} \end{bmatrix},$$
(54)

in which we recall that F_i is the thrust of the *i*th quadrotor. Here, for any designated reference yaw signal ψ_{di} satisfying Assumption 1, we define ([25])

$$F_i = ||u_i||, \tag{55}$$

$$\phi_{di} = \arcsin\left(\frac{u_{i1}s\psi_{di} - u_{i2}c\psi_{di}}{||u_i||}\right),\tag{56}$$

$$\theta_{di} = \arctan\left(\frac{u_{i1}c\psi_{di} + u_{i2}s\psi_{di}}{u_{i3}}\right),\tag{57}$$

where $u_i = [u_{i1}, u_{i2}, u_{i3}]^T \in \mathbb{R}^3$, with ϕ_{di} and θ_{di} satisfying Assumption 2.

Let $V_3 = \sum_{i=1}^N \frac{1}{2} e_{\Theta i}^{\mathrm{T}} e_{\Theta i}$, which has the following time derivative

$$\dot{V}_{3} = \sum_{i=1}^{N} e_{\Theta i}^{\mathrm{T}} \dot{e}_{\Theta i} = \sum_{i=1}^{N} e_{\Theta i}^{\mathrm{T}} (T_{i} e_{\omega_{i}} + T_{i} \alpha_{\Theta i} - \dot{\Theta}_{\mathrm{d}i}), \quad (58)$$

where we define $e_{\omega i} = \omega_i - \alpha_{\Theta i}$ $(i = 1, \dots, N)$, with the stabilizing function $\alpha_{\Theta i} \in \mathbb{R}^3$ designed in (42). Taking derivative of $\phi_{\mathrm{d}i}$ in (56) and $\theta_{\mathrm{d}i}$ in (57) with respect to time yields

$$\dot{\phi}_{di} = \frac{\partial \phi_{di}}{\partial u_{i1}} \dot{u}_{i1} + \frac{\partial \phi_{di}}{\partial u_{i2}} \dot{u}_{i2} + \frac{\partial \phi_{di}}{\partial u_{i3}} \dot{u}_{i3} + \frac{\partial \phi_{di}}{\partial \psi_{di}} \dot{\psi}_{di},
\dot{\theta}_{di} = \frac{\partial \theta_{di}}{\partial u_{i1}} \dot{u}_{i1} + \frac{\partial \theta_{di}}{\partial u_{i2}} \dot{u}_{i2} + \frac{\partial \theta_{di}}{\partial u_{i3}} \dot{u}_{i3} + \frac{\partial \theta_{di}}{\partial \psi_{di}} \dot{\psi}_{di},$$

where u_{i1} , u_{i2} , u_{i3} , ψ_{di} , and $\dot{\psi}_{di}$ are all bounded according to Theorem 1 and Assumption 2, such that terms $\frac{\partial \phi_{di}}{\partial u_{i1}}$, $\frac{\partial \phi_{di}}{\partial u_{i2}}$, $\frac{\partial \phi_{di}}{\partial u_{i2}}$, $\frac{\partial \phi_{di}}{\partial u_{i3}}$, and $\frac{\partial \theta_{di}}{\partial \psi_{di}}$ are all bounded. The result of differentiating u_i in (26) with respect to time can be combined with Theorem 1 to conclude the boundedness of \dot{u}_{i1} , \dot{u}_{i2} , and \dot{u}_{i3} . Therefore, $\dot{\Theta}_{di}$ is bounded, which satisfies $||\dot{\Theta}_{di}|| \leq \bar{\Theta}_{di}$, where $\bar{\Theta}_{di}$ is an $\underline{unknown}$ positive constant. Note that for any $v_i > 0$,

$$e_{\Theta i}^{\mathrm{T}} \dot{\Theta}_{\mathrm{d}i} \leq ||e_{\Theta i}|| \, \bar{\Theta}_{\mathrm{d}i} < \frac{1}{\nu_i} \bar{\Theta}_{\mathrm{d}i}^2 + \nu_i \, ||e_{\Theta i}||^2 \,.$$

Therefore, from (58) we can get

$$\dot{V}_{3} < \sum_{i=1}^{N} \left(-K_{\Theta i} e_{\Theta i}^{\mathsf{T}} e_{\Theta i} + e_{\Theta i}^{\mathsf{T}} T_{i} e_{\omega i} + \frac{1}{\nu_{i}} \bar{\Theta}_{\mathrm{d}i}^{2} \right). \tag{59}$$

APPENDIX C STEP 4 OF BACKSTEPPING DESIGN

Taking derivative of $V_4 = \sum_{i=1}^N \frac{1}{2} e_{\omega i}^{\rm T} e_{\omega i}$ with respect to time yields

$$\dot{V}_{4} = \sum_{i=1}^{N} e_{\omega i}^{\mathrm{T}} (J_{i}^{-1} \mathbb{S}(J_{i} \omega_{i}) \omega_{i} + J_{i}^{-1} \tau_{i} - \dot{\alpha}_{\Theta i} + J_{i}^{-1} \gamma_{2i}),$$
(60)

where, from (42), we can get

$$\dot{\alpha}_{\Theta i} = -(K_{\Theta i} + \nu_i) \left(\frac{\mathrm{d}(T_i^{-1})}{\mathrm{d}t} e_{\Theta i} + \omega_i - T_i^{-1} \dot{\Theta}_{\mathrm{d}i} \right).$$

$$\bar{J}_{i} = \begin{bmatrix} \bar{J}_{1i}, & \bar{J}_{2i}, & \bar{J}_{3i}, & \bar{J}_{4i}, & \bar{J}_{5i}, & \bar{J}_{6i} \end{bmatrix}, \qquad \text{with}$$

$$\bar{J}_{1i} = \begin{bmatrix} \varsigma_{xyi} J_{zxi} - \varsigma_{xzi} J_{yxi} \\ \varsigma_{yyi} J_{zxi} - \varsigma_{yzi} J_{yxi} \\ \varsigma_{zyi} J_{zxi} - \varsigma_{zzi} J_{yxi} \end{bmatrix}, \quad \bar{J}_{2i} = \begin{bmatrix} -\varsigma_{xxi} J_{zxi} + \varsigma_{xyi} J_{zyi} + \varsigma_{xzi} (J_{xxi} - J_{yyi}) \\ -\varsigma_{yxi} J_{zxi} + \varsigma_{yyi} J_{zyi} + \varsigma_{yzi} (J_{xxi} - J_{yyi}) \end{bmatrix},$$

$$\bar{J}_{3i} = \begin{bmatrix} \varsigma_{xxi} J_{yxi} + \varsigma_{xyi} (J_{zzi} - J_{xxi}) - \varsigma_{xzi} J_{yzi} \\ \varsigma_{yxi} J_{yxi} + \varsigma_{yyi} (J_{zzi} - J_{xxi}) - \varsigma_{yzi} J_{yzi} \\ \varsigma_{zxi} J_{yxi} + \varsigma_{zzi} (J_{zxi} - J_{xxi}) - \varsigma_{zzi} J_{yzi} \end{bmatrix}, \quad \bar{J}_{4i} = \begin{bmatrix} -\varsigma_{xxi} J_{zyi} + \varsigma_{xzi} J_{xyi} \\ -\varsigma_{xxi} J_{zyi} + \varsigma_{zzi} J_{xyi} \\ -\varsigma_{xxi} J_{zyi} + \varsigma_{zzi} J_{xyi} \end{bmatrix},$$

$$\bar{J}_{5i} = \begin{bmatrix} \varsigma_{xxi} (J_{yyi} - J_{zzi}) - \varsigma_{xyi} J_{xyi} + \varsigma_{xzi} J_{xzi} \\ \varsigma_{yxi} (J_{yyi} - J_{zzi}) - \varsigma_{yyi} J_{xyi} + \varsigma_{zzi} J_{xzi} \\ \varsigma_{zxi} (J_{yyi} - J_{zzi}) - \varsigma_{zyi} J_{xyi} + \varsigma_{zzi} J_{xzi} \end{bmatrix}, \quad \bar{J}_{6i} = \begin{bmatrix} \varsigma_{xxi} J_{yzi} - \varsigma_{xyi} J_{xzi} \\ \varsigma_{xxi} J_{yzi} - \varsigma_{yyi} J_{xzi} \\ \varsigma_{zxi} J_{yzi} - \varsigma_{zyi} J_{xzi} \end{bmatrix},$$

where

$$J_{i} = \begin{bmatrix} J_{xxi} & J_{xyi} & J_{xzi} \\ J_{yxi} & J_{yyi} & J_{yzi} \\ J_{zxi} & J_{zyi} & J_{zzi} \end{bmatrix}, \quad J_{i}^{-1} = \begin{bmatrix} \varsigma_{xxi} & \varsigma_{xyi} & \varsigma_{xzi} \\ \varsigma_{yxi} & \varsigma_{yyi} & \varsigma_{yzi} \\ \varsigma_{zxi} & \varsigma_{zyi} & \varsigma_{zzi} \end{bmatrix},$$

and

$$\bar{\omega}_i = \begin{bmatrix} \omega_{xi}^2, & \omega_{xi}\omega_{yi}, & \omega_{xi}\omega_{zi}, & \omega_{yi}^2, & \omega_{yi}\omega_{zi}, & \omega_{zi}^2 \end{bmatrix}^{\mathrm{T}}.$$
 (63)

Hence \dot{V}_4 can be rewritten as

$$\dot{V}_{4} = \sum_{i=1}^{N} e_{\omega i}^{T} \left[J_{i}^{-1} \mathbb{S}(J_{i}\omega_{i})\omega_{i} + J_{i}^{-1}\tau_{i} + J_{i}^{-1}\gamma_{2i} + (K_{\Theta i} + \nu_{i}) \left(\frac{d(T_{i}^{-1})}{dt} e_{\Theta i} + \omega_{i} - T_{i}^{-1} \dot{\Theta}_{di} \right) \right], \quad (61)$$

where $T_i^{-1}\dot{\Theta}_{\mathrm{d}i}$ is bounded since $\dot{\Theta}_{\mathrm{d}i}$ and $\left|\left|T_i^{-1}\right|\right|$ are both bounded. Note that we can further parameterize the term $e_{\omega i}^{\mathrm{T}}J_i^{-1}\mathbb{S}(J_i\omega_i)\omega_i$ as $e_{\omega i}^{\mathrm{T}}J_i^{-1}\mathbb{S}(J_i\omega_i)\omega_i=e_{\omega i}^{\mathrm{T}}\bar{J}_i\bar{\omega}_i$, where \bar{J}_i and $\bar{\omega}_i$ for the ith quadrotor $(i=1,\cdots,N)$ are defined in (62) and (63), as shown at the top of the page. Here \bar{J}_i is an $\underline{unknown}$ constant matrix, and there exists an $\underline{unknown}$ constant $\bar{h}_{\bar{J}i}$ satisfying $w_1^{\mathrm{T}}\bar{J}_iw_2\leq ||w_1||\,\bar{h}_{\bar{J}i}\,||w_2||$ for any $w_1\in\mathbb{R}^3$ and $w_2\in\mathbb{R}^6$.

Therefore, we have

$$e_{\omega i}^{\mathsf{T}} J_{i}^{-1} \mathbb{S}(J_{i}\omega_{i})\omega_{i} \leq ||e_{\omega i}|| \,\bar{h}_{\bar{J}i} \,||\bar{\omega}_{i}||$$

$$< \varepsilon_{i} \bar{h}_{\bar{J}i} + \bar{h}_{\bar{J}i} \frac{e_{\omega i}^{\mathsf{T}} e_{\omega i} \bar{\omega}_{i}^{\mathsf{T}} \bar{\omega}_{i}}{\sqrt{e_{\omega i}^{\mathsf{T}} e_{\omega i} \bar{\omega}_{i}^{\mathsf{T}} \bar{\omega}_{i} + \varepsilon_{i}^{2}}}.$$
 (64)

Besides.

$$e_{\omega i}^{\mathsf{T}} \left(J_{i}^{-1} \gamma_{2i} - (K_{\Theta i} + \nu_{i}) T_{i}^{-1} \dot{\Theta}_{\mathrm{d}i} \right)$$

$$\leq ||e_{\omega i}|| \, \mu_{Ji} < \varepsilon_{i} \mu_{Ji} + \mu_{Ji} \frac{e_{\omega i}^{\mathsf{T}} e_{\omega i}}{\sqrt{e_{\omega i}^{\mathsf{T}} e_{\omega i} + \varepsilon_{i}^{2}}}, \tag{65}$$

where μ_{Ji} is an $\underline{unknown}$ constant satisfying $\left| \left| J_i^{-1} \gamma_{2i} - (K_{\Theta i} + \nu_i) T_i^{-1} \dot{\Theta}_{di} \right| \right| \leq \mu_{Ji}$.

ACKNOWLEDGMENT

The authors appreciate the Editor-in-Chief, Associate Editor, and Reviewers from IEEE TRANSACTIONS ON INTELLI-

GENT TRANSPORTATION SYSTEMS for the helpful comments and constructive suggestions during the review process.

REFERENCES

- [1] T. J. Koo and S. M. Shahruz, "Formation of a group of unmanned aerial vehicles (UAVs)," in *Proc. Amer. Control Conf.*, 2001, pp. 69–74.
- [2] T. Kopfstedt, M. Mukai, M. Fujita, and C. Ament, "Control of formations of UAVs for surveillance and reconnaissance missions," *IFAC Proc. Volumes*, vol. 41, no. 2, pp. 5161–5166, 2008.
- [3] J. Scherer et al., "An autonomous multi-UAV system for search and rescue," in *Proc. 1st Workshop Micro Aerial Vehicle Netw.*, Syst., Appl. Civilian Use, May 2015, pp. 33–38.
- [4] J. Han, Y. Xu, L. Di, and Y. Chen, "Low-cost multi-UAV technologies for contour mapping of nuclear radiation field," *J. Intell. Robotic Syst.*, vol. 70, nos. 1–4, pp. 401–410, Apr. 2013.
- [5] J. Han and Y. Chen, "Multiple UAV formations for cooperative source seeking and contour mapping of a radiative signal field," *J. Intell. Robot.* Syst., vol. 74, no. 1, pp. 323–332, 2014.
- [6] J. Zhang et al., "PSO-based sparse source location in large-scale environments with a UAV swarm," *IEEE Trans. Intell. Transp. Syst.*, vol. 24, no. 5, pp. 5249–5258, May 2023.
- [7] N. S. Zú niga, F. Mu noz, M. A. Márquez, E. S. Espinoza, and L. R. G. Carrillo, "Load transportation using single and multiple quadrotor aerial vehicles with swing load attenuation," in *Proc. Int. Conf. Unmanned Aircr. Syst. (ICUAS)*, Jun. 2018, pp. 269–278.
- [8] K. Klausen, C. Meissen, T. I. Fossen, M. Arcak, and T. A. Johansen, "Cooperative control for multirotors transporting an unknown suspended load under environmental disturbances," *IEEE Trans. Control Syst. Technol.*, vol. 28, no. 2, pp. 653–660, Mar. 2020.
- [9] X. Jin and Z. Hu, "Adaptive cooperative load transportation by a team of quadrotors with multiple constraint requirements," *IEEE Trans. Intell. Transp. Syst.*, vol. 24, no. 1, pp. 801–814, Jan. 2023.
- [10] Y. Wang, G. Yu, W. Xie, W. Zhang, and C. Silvestre, "Cooperative path following control of a team of quadrotor-slung-load systems under disturbances," *IEEE Trans. Intell. Vehicles*, vol. 8, no. 9, pp. 4169–4179, Sep. 2023.
- [11] Y. Wang, G. Yu, W. Xie, W. Zhang, and C. Silvestre, "Robust cooperative transportation of a cable-suspended payload by multiple quadrotors featuring cable-reconfiguration capabilities," *IEEE Trans. Intell. Transp. Syst.*, vol. 25, no. 9, pp. 11833–11843, Sep. 2024.
- [12] K. Sigurd and J. How, "UAV trajectory design using total field collision avoidance," in *Proc. AIAA Guid.*, *Navigat.*, *Control Conf. Exhib.*, Aug. 2003, p. 5728.

- [13] R. K. Sharma and D. Ghose, "Collision avoidance between UAV clusters using swarm intelligence techniques," *Int. J. Syst. Sci.*, vol. 40, no. 5, pp. 521–538, May 2009.
- [14] A. Alexopoulos, A. Kandil, P. Orzechowski, and E. Badreddin, "A comparative study of collision avoidance techniques for unmanned aerial vehicles," in *Proc. IEEE Int. Conf. Syst., Man, Cybern.*, Oct. 2013, pp. 1969–1974.
- [15] Y. Kuriki and T. Namerikawa, "Consensus-based cooperative formation control with collision avoidance for a multi-UAV system," in *Proc. Amer. Control Conf.*, Jun. 2014, pp. 2077–2082.
- [16] A. Moses, M. J. Rutherford, M. Kontitsis, and K. P. Valavanis, "UAV-borne X-band radar for collision avoidance," *Robotica*, vol. 32, no. 1, pp. 97–114, Jan. 2014.
- [17] J. Goricanec, A. Milas, L. Markovic, and S. Bogdan, "Collision-free trajectory following with augmented artificial potential field using UAVs," *IEEE Access*, vol. 11, pp. 83492–83506, 2023.
- [18] L. Wang, A. D. Ames, and M. Egerstedt, "Safe certificate-based maneuvers for teams of quadrotors using differential flatness," in *Proc. IEEE Int. Conf. Robot. Autom. (ICRA)*, May 2017, pp. 3293–3298.
- [19] L. Balandi, N. De Carli, and P. R. Giordano, "Persistent monitoring of multiple moving targets using high order control barrier functions," *IEEE Robot. Autom. Lett.*, vol. 8, no. 8, pp. 5236–5243, Aug. 2023.
- [20] S. Wang, Y. Wang, Z. Miao, X. Wang, and W. He, "Dual model predictive control of multiple quadrotors with formation maintenance and collision avoidance," *IEEE Trans. Ind. Electron.*, vol. 71, no. 12, pp. 16037–16046, Dec. 2024.
- [21] M. Wei, L. Zheng, Y. Wu, H. Liu, and H. Cheng, "Safe learning-based control for multiple UAVs under uncertain disturbances," *IEEE Trans. Autom. Sci. Eng.*, vol. 21, no. 4, pp. 7349–7362, Oct. 2024.
- [22] S. Wu, T. Liu, M. Egerstedt, and Z.-P. Jiang, "Quadratic programming for continuous control of safety-critical multiagent systems under uncertainty," *IEEE Trans. Autom. Control*, vol. 68, no. 11, pp. 6664–6679, Nov. 2023.
- [23] E. Restrepo, A. Loría, I. Sarras, and J. Marzat, "Robust consensus of high-order systems under output constraints: Application to rendezvous of underactuated UAVs," *IEEE Trans. Autom. Control*, vol. 68, no. 1, pp. 329–342, Jan. 2023.
- [24] B. Zhu, M. Chen, and T. Li, "Prescribed performance-based tracking control for quadrotor UAV under input delays and input saturations," *Trans. Inst. Meas. Control*, vol. 44, no. 10, pp. 2049–2062, Jun. 2022.
- [25] Z. Zuo and C. Wang, "Adaptive trajectory tracking control of output constrained multi-rotors systems," *IET Control Theory Appl.*, vol. 8, no. 13, pp. 1163–1174, Sep. 2014.
- [26] Y. Xia, X. Shao, Z. Mei, and W. Zhang, "Performance-designated reinforcement learning enclosing control for UAVs with collisionfree capability," *IEEE Trans. Intell. Transp. Syst.*, vol. 25, no. 9, pp. 12644–12656, Sep. 2024.
- [27] Z. Hu and X. Jin, "Adaptive formation control architectures for a team of quadrotors with multiple performance and safety constraints," *Int. J. Robust Nonlinear Control*, vol. 33, no. 14, pp. 8183–8204, Sep. 2023.
- [28] G. Li, X. Wang, Z. Zuo, Y. Wu, and J. Lü, "Fault-tolerant formation control for leader-follower flight vehicles under malicious attacks," *IEEE Trans. Intell. Vehicles*, early access, Apr. 22, 2024.
- [29] F. Borrelli, T. Keviczky, and G. J. Balas, "Collision-free UAV formation flight using decentralized optimization and invariant sets," in *Proc. 43rd IEEE Conf. Decis. Control (CDC)*, vol. 1, Dec. 2004, pp. 1099–1104.
- [30] X. Wang, V. Yadav, and S. N. Balakrishnan, "Cooperative UAV formation flying with obstacle/collision avoidance," *IEEE Trans. Control Syst. Technol.*, vol. 15, no. 4, pp. 672–679, Jul. 2007.
- [31] C. Luo, S. I. McClean, G. Parr, L. Teacy, and R. De Nardi, "UAV position estimation and collision avoidance using the extended Kalman filter," *IEEE Trans. Veh. Technol.*, vol. 62, no. 6, pp. 2749–2762, Jul. 2013.
- [32] P. Pierpaoli and A. Rahmani, "UAV collision avoidance exploitation for noncooperative trajectory modification," *Aerosp. Sci. Technol.*, vol. 73, pp. 173–183, Feb. 2018.
- [33] Y. Chen, M. Guo, and Z. Li, "Deadlock resolution and recursive feasibility in MPC-based multirobot trajectory generation," *IEEE Trans. Autom. Control*, vol. 69, no. 9, pp. 6058–6073, Sep. 2024.
- [34] X. Jin, S.-L. Dai, and J. Liang, "Fixed-time path-following control of an autonomous vehicle with path-dependent performance and feasibility constraints," *IEEE Trans. Intell. Veh.*, vol. 8, no. 1, pp. 458–468, Jan. 2023.
- [35] R. W. Beard and T. W. McLain, Small Unmanned Aircraft: Theory and Practice. Princeton, NJ, USA: Princeton Univ. Press, 2012.

- [36] K. D. Do, Z. P. Jiang, and J. Pan, "Robust adaptive path following of underactuated ships," *Automatica*, vol. 40, no. 6, pp. 929–944, Jun. 2004.
- [37] X. Jin, "Fault-tolerant iterative learning control for mobile robots non-repetitive trajectory tracking with output constraints," *Automatica*, vol. 94, pp. 63–71, Aug. 2018.
- [38] S.-L. Dai, S. He, M. Wang, and C. Yuan, "Adaptive neural control of underactuated surface vessels with prescribed performance guarantees," *IEEE Trans. Neural Netw. Learn. Syst.*, vol. 30, no. 12, pp. 3686–3698, Dec. 2019.
- [39] A. P. Aguiar and J. P. Hespanha, "Trajectory-tracking and path-following of underactuated autonomous vehicles with parametric modeling uncertainty," *IEEE Trans. Autom. Control*, vol. 52, no. 8, pp. 1362–1379, Aug. 2007.
- [40] J. Ghommam and F. Mnif, "Coordinated path-following control for a group of underactuated surface vessels," *IEEE Trans. Ind. Electron.*, vol. 56, no. 10, pp. 3951–3963, Oct. 2009.
- [41] X. Jin, "Adaptive fault tolerant tracking control for a class of stochastic nonlinear systems with output constraint and actuator faults," Syst. Control Lett., vol. 107, pp. 100–109, Sep. 2017.
- [42] W. Xie, W. Zhang, and C. Silvestre, "Saturated backstepping-based tracking control of a quadrotor with uncertain vehicle parameters and external disturbances," *IEEE Control Syst. Lett.*, vol. 6, pp. 1634–1639, 2022.
- [43] H. Liu, W. Zhao, and J. Xi, "Optimal formation control for a quadrotor team under switching topologies via reinforcement learning," in *Proc. 4th IEEE Int. Conf. Ind. Cyber-Phys. Syst. (ICPS)*, May 2021, pp. 731–736.
- [44] X. Jin, "Adaptive fixed-time control for MIMO nonlinear systems with asymmetric output constraints using universal barrier functions," *IEEE Trans. Autom. Control*, vol. 64, no. 7, pp. 3046–3053, Jul. 2019.
- [45] K. P. Tee, S. S. Ge, and E. H. Tay, "Barrier Lyapunov functions for the control of output-constrained nonlinear systems," *Automatica*, vol. 45, no. 4, pp. 918–927, Apr. 2009.
- [46] X. Jin and J.-X. Xu, "Iterative learning control for output-constrained systems with both parametric and nonparametric uncertainties," *Automatica*, vol. 49, no. 8, pp. 2508–2516, Aug. 2013.
- [47] C. Wang and Y. Lin, "Decentralized adaptive tracking control for a class of interconnected nonlinear time-varying systems," *Automatica*, vol. 54, pp. 16–24, Apr. 2015.
- [48] Z. Wang, Y. Zou, Y. Liu, and Z. Meng, "Distributed control algorithm for leader-follower formation tracking of multiple quadrotors: Theory and experiment," *IEEE/ASME Trans. Mechatronics*, vol. 26, no. 2, pp. 1095–1105, Apr. 2021.



Zhongjun Hu received the B.Eng. degree in automation from the College of Information Engineering, Zhejiang University of Technology, Hangzhou, China, in 2018, and the M.S. degree in electrical and computer engineering from The Ohio State University, Columbus, OH, USA, in 2020. He is currently pursuing the Ph.D. degree with the Department of Mechanical and Aerospace Engineering, University of Kentucky, Lexington, KY, USA.

His research interests include adaptive control and its application of multi-agent systems.



Xu Jin (Member, IEEE) received the B.Eng. degree (Hons.) in electrical and computer engineering from the National University of Singapore, Singapore, the M.A.Sc. degree in electrical and computer engineering from the University of Toronto, Toronto, ON, Canada, and the M.S. degree in mathematics and the Ph.D. degree in aerospace engineering from Georgia Institute of Technology, Atlanta, GA, USA.

He is currently an Assistant Professor with the Department of Mechanical and Aerospace Engineering, University of Kentucky, Lexington, KY, USA.

His current research interests include adaptive and iterative learning control, with applications to intelligent vehicles, autonomous robots, and nonlinear multiagent systems. He was a recipient of the NSF CAREER Award in 2024.